CMS-BPH-15-005

Measurement of quarkonium production cross sections in pp collisions at $\sqrt{s} = 13\,\text{TeV}$

The CMS Collaboration[*]

Abstract

Differential production cross sections of J/ψ and ψ(2S) charmonium and Y(nS) (n = 1, 2, 3) bottomonium states are measured in proton-proton collisions at $\sqrt{s} = 13\,\text{TeV}$, with data collected by the CMS detector at the LHC, corresponding to an integrated luminosity of $2.3\,\text{fb}^{-1}$ for the J/ψ and $2.7\,\text{fb}^{-1}$ for the other mesons. The five quarkonium states are reconstructed in the dimuon decay channel, for dimuon rapidity $|y| < 1.2$. The double-differential cross sections for each state are measured as a function of y and transverse momentum, and compared to theoretical expectations. In addition, ratios are presented of cross sections for prompt ψ(2S) to J/ψ, Y(2S) to Y(1S), and Y(3S) to Y(1S) production.

Submitted to Physics Letters B

[*]See Appendix B for the list of collaboration members

1 Introduction

Since the discovery of heavy-quark bound states, quarkonium production in hadronic collisions has been the subject of many theoretical and experimental studies. A well established theoretical framework to describe quarkonium production is nonrelativistic quantum chromodynamics (NRQCD) [1–3], an effective theory that assumes that the mechanism can be factorized in two steps. In the first step, a heavy quark-antiquark pair is produced in a given spin and orbital angular momentum state, either in a color-singlet or color-octet configuration. The corresponding parton-level cross sections, usually called short-distance coefficients (SDCs), are functions of the kinematics of the state and can be calculated perturbatively, presently up to next-to-leading order (NLO) [4–7]. In the second step, the quark-antiquark pairs bind into the final quarkonium states through a nonperturbative hadronization process, with transition probabilities determined by process-independent long-distance matrix elements (LDMEs). Unlike the SDCs, the LDMEs are presently not calculable and must be obtained through fits to experimental data [4–9]. Until recently, for directly produced S-wave quarkonia, the color-octet $^{3}S_{1}$ term was thought to dominate, which would result in a strong transverse polarization of the mesons relative to their direction of motion (helicity frame) at large transverse momentum, p_{T}.

Experiments at the CERN LHC have provided measurements of the production of the S-wave quarkonium states $\eta_{c}(1S)$, J/ψ, $\psi(2S)$, and Y(nS) (n = 1, 2, 3), and of the P-wave states, $\chi_{c1,2}$ and $\chi_{b1,2}(1P)$ [10–14], at center-of-mass energies of 2.76, 7 and 8 TeV. These measurements of the S-wave states include both the differential cross sections [15–28] and polarizations [29–33], and offer strong indication that, contrary to previous expectations, these mesons are produced unpolarized. Further theoretical and experimental work can provide deeper insights on how to interpret these observations. In particular, additional data can help in improving the fits and determine more precisely the relative weights of the LDMEs.

We report the measurement of double-differential cross sections of the five S-wave quarkonium states J/ψ, $\psi(2S)$, and Y(nS) in pp collisions at $\sqrt{s} = 13$ TeV by the CMS detector at the LHC. The increased center-of-mass energy and production cross sections provide an extended reach in p_{T} and improved statistical precision relative to similar measurements at 7 TeV [23–26, 34]. The measurements performed at 13 TeV also provide the opportunity to test the $\sqrt{s}$ dependence of the cross sections and to check the validity of the factorization hypothesis and LDME universality implied in NRQCD.

The product of the branching fraction of quarkonia to muon pairs, $\mathcal{B}(\mathcal{Q} \rightarrow \mu^{+}\mu^{-})$, and the double-differential production cross section, $\mathrm{d}^{2}\sigma/(\mathrm{d}p_{T}\,\mathrm{d}y)$, in bins of p_{T} and rapidity, y, is given by

$$\mathcal{B}(\mathcal{Q} \rightarrow \mu^{+}\mu^{-})\frac{\mathrm{d}^{2}\sigma}{\mathrm{d}p_{T}\,\mathrm{d}y} = \frac{N(p_{T},y)}{\mathcal{L}\Delta y\Delta p_{T}}\left\langle \frac{1}{\epsilon(p_{T},y)\mathcal{A}(p_{T},y)}\right\rangle, \tag{1}$$

where $N(p_{T}, y)$ is the number of prompt signal events in the bin, $\mathcal{L}$ is the integrated luminosity, Δy and Δp_{T} are the bin widths, and $\langle 1/(\epsilon(p_{T},y)\mathcal{A}(p_{T},y))\rangle$ represents the average of the product of the inverse acceptance and efficiency for all the events in the bin. Only prompt signal events are considered. The nonprompt components of the J/ψ and $\psi(2S)$ mesons, i.e. originating from decays of b hadrons, are separated using the decay length defined as $\ell = L_{xy} \cdot m/p_{T}$, where L_{xy} is the distance measured in the transverse plane between the average location of the luminous region and the fitted position of the dimuon vertex, m is the mass of the J/ψ ($\psi(2S)$) from Ref. [35], and p_{T} the transverse momentum of the dimuon candidate. For the prompt signal events, we do not distinguish between feed-down decays of heavier quarkonium states and directly produced quarkonia.

2   The CMS detector, data set, and event selection

The analysis uses dimuon events collected in pp collisions at $\sqrt{s} = 13\,\text{TeV}$ with the CMS detector. The central feature of the CMS apparatus is a superconducting solenoid of 6 m internal diameter, providing a magnetic field of 3.8 T. Within the solenoid volume are a silicon pixel and strip tracker, a lead tungstate crystal electromagnetic calorimeter, and a brass and scintillator hadron calorimeter, each composed of a barrel and two endcap sections. Forward calorimeters extend the pseudorapidity (η) coverage provided by the barrel and endcap detectors. Muons are detected in gas-ionization chambers embedded in the steel flux-return yoke outside the solenoid [36]. A more detailed description of the CMS detector, together with a definition of the coordinate system used and the relevant kinematic variables, can be found in Ref. [37].

The data were collected using a multilevel trigger system [38]. The first level (L1), made of custom hardware processors providing coarse momentum information, requires two muons within the range $|\eta| < 1.6$. Second (L2) and third (L3) levels, collectively known as the HLT (High-Level Trigger), are implemented in software. At these levels, the muon selection is refined, then opposite-charge muon candidates are paired and required to have an invariant mass in the regions 2.9–3.3, 3.35–4.05, or 8.5–11 GeV for the J/ψ, ψ(2S), and Y(nS), respectively. The dimuon p_T is required to be above 9.9 GeV for the J/ψ and above 7.9 GeV for the remaining states. For all five states, the dimuon rapidity is restricted to $|y| < 1.25$. A fit of the positions and momenta of the two muon candidates to a common vertex is performed, and the fit χ^2 probability is required to be above 0.5%. The sample collected with these triggers has a total integrated luminosity of $2.3\,\text{fb}^{-1}$ for the J/ψ and $2.7\,\text{fb}^{-1}$ for the other mesons. The lower value for the J/ψ is the consequence of the trigger prescaling that was applied to limit the rate during part of the data taking.

When reconstructing the five states offline, further requirements are applied: only muons with $p_\text{T}^\mu > 4.5$ GeV in the range $|\eta^\mu| < 0.3$, or $p_\text{T}^\mu > 4.0$ GeV in the range $0.3 < |\eta^\mu| < 1.4$ are selected. The muons have to match the triggered pair and be identified as reconstructed tracks with at least five measurements in the silicon tracker and at least one in the pixel detector. The track is required to match at least one muon segment identified by a muon detector plane. Loose criteria are applied on the longitudinal and transverse impact parameters to reject cosmic rays and in-flight hadron decays. The dimuon vertex χ^2 probability is required to be greater than 1%. In the CMS magnetic field, the two muons can bend towards or away from each other; only the second type of event is considered in this analysis since the first type exhibits high trigger inefficiencies. The dimuon rapidity is restricted to $|y| < 1.2$.

The double-differential cross sections are presented in four (two) rapidity bins for the prompt J/ψ and ψ(2S) (Y(nS)), and in several bins of p_T, covering a p_T range between 20 and 120 (100) GeV for J/ψ (ψ(2S), Y(nS)), extending up to 150 (130) GeV for measurements integrated in rapidity.

3   Acceptance and efficiencies

The acceptance is calculated using simulated events produced with a single-particle event generator. The quarkonium states are generated with a flat y distribution and a realistic p_T distribution derived from data [24, 25], covering the analysis phase space. The PYTHIA 8.205 [39] Monte Carlo event generator is used to produce an unpolarized dimuon decay (corresponding to a flat dimuon angular distribution), also accounting for final-state photon radiation. The simulated events include multiple proton-proton interactions in the same or nearby beam crossings (pileup), with the distribution matching that observed in data, with an average of about 11 col-

lisions per bunch crossing. The acceptance for events in a given $(p_T, |y|)$ range is defined as the ratio of the number of generated events that pass the kinematic selection criteria described above to the total number of simulated events in that p_T and $|y|$ range. The acceptance depends on the quarkonium polarization. It is derived for the unpolarized scenario, which is compatible with experimental measurements within uncertainties. We also calculate multiplicative correction factors that allow, from the unpolarized case, to infer the acceptance that corresponds to three different values of the polar anisotropy parameter, $\lambda_\theta^{\mathrm{HX}}$, in the helicity frame: -1 (fully longitudinal), $+1$ (fully transverse), and k, with k reflecting the CMS measured value of $\lambda_\theta^{\mathrm{HX}}$ for each quarkonium state [30, 31], also used in Refs. [25, 26]. The multiplicative factors to convert the cross sections calculated using the unpolarized scenario to the ones calculated employing one of the polarization scenarios described above are provided.

The single-muon trigger, reconstruction, and identification efficiencies are measured individually from data as a function of muon p_T and $|\eta|$, applying a tag-and-probe [23, 34] technique on J/ψ and Y(1S) candidates acquired with triggers that are independent from those used for the measurements of the yields. The individual efficiencies are multiplied and then parameterized using a sigmoid function. The dimuon efficiency is obtained as the product of the efficiencies of the two muons, multiplied by a correction factor, ρ, that takes into account the correlation between the two muons. The ρ factor is derived from data, using a trigger, independent from the ones used for the measurement of the yield, requiring a single muon at L1. ρ becomes increasingly important with higher dimuon p_T, when the two muons are close to each other in space, causing the efficiency to decrease. Dimuon efficiencies are around 85% for the J/ψ and ψ(2S) up to a dimuon p_T of 50 GeV and decrease slowly for higher p_T due to the ρ factor. In the case of the Y(nS) states, the dimuon efficiencies are nearly constant around 90%. The acceptance and efficiency term in Eq. (1) is obtained by averaging the values of the inverse of the acceptance times efficiency for all the individual dimuon candidates in each p_T and $|y|$ range.

4 Determination of the yields

The signal and background yields are obtained through an extended unbinned maximum-likelihood fit to the dimuon invariant mass distribution in the case of the Y(nS) states, and to the dimuon invariant mass and decay length distributions for the J/ψ and ψ(2S) mesons. In both cases, the number of signal and background candidates are free parameters in the fit.

The three Y(nS) signal peaks are modeled with Crystal Ball (CB) functions [40], composed of a Gaussian core, characterized by a mean m, a width σ_m, and a tail characterized by two parameters, n and α. The CB function is used to account for the energy loss due to the final-state radiation of the muons. The mean mass values are fixed to those of the Particle Data Group [35], multiplied by a common factor that calibrates the mass scale, left as a free parameter in the fit. The width of the CB function is a free parameter only in the case of the Y(1S), while the width of the CB functions describing the Y(2S) and Y(3S) peaks are fixed to the width of the Y(1S), scaled by the ratio of their masses to the mass of the Y(1S). The Y(nS) dimuon mass resolution σ_m is a function of rapidity and spans the range 60 to 90 MeV for $|y| < 1.2$ in the case of the Y(1S). The tail parameters n and α are the same for all three CB functions; n is fixed and α is constrained to a Gaussian probability distribution. Both constraints are derived from a fit of the Y(1S) dimuon invariant mass shape, using the p_T-integrated distribution to reduce the statistical fluctuations. The background is modeled using an exponential function.

For the J/ψ and ψ(2S) mesons, an additional nonprompt component originating from the decay of b hadrons must be taken into account. The prompt and nonprompt yields are measured by fitting the dimuon invariant mass and decay length distributions. The J/ψ dimuon invariant

mass distribution is modeled by the sum of a CB and a Gaussian function with common mean, while the corresponding $\psi(2S)$ distribution is described using only a CB function. The widths of the CB and Gaussian functions, as well as the α of the CB functions, are free parameters. The σ_m varies as a function of rapidity between 20 and 50 (40) MeV for the J/ψ ($\psi(2S)$) state. The m and n parameters are fixed to values derived from fits to the invariant mass distribution of the p_T-integrated data. An exponential is used to describe the dimuon mass background. The decay length distribution is modeled by a prompt signal component represented by a resolution function, a nonprompt term given by an exponential function convolved with the resolution function, and a background term represented by the sum of a resolution function plus an exponential decay function to take into account prompt and nonprompt background components. The resolution function is modeled by the sum of two Gaussian functions whose widths are taken as the event-by-event decay length uncertainty, multiplied by global scale factors. The two scale factors are free parameters in the fit and are constrained with Gaussian probability distributions that are derived from fits to the p_T-integrated data, less affected by statistical fluctuations. The effective width of the two Gaussian functions is approximately 25 μm.

To verify that the fits to the quarkonium states are unbiased and the uncertainties are correctly modeled, 1000 pseudo-experiments were produced from simulation. Similarly, simulated events were used to test the hypotheses made on the constraints of the parameters. Differences in the event-by-event uncertainty information between signal and background candidates could introduce biases in the fitting of the decay length using the simplified model described above, but we verified that these effects are negligible. Examples of fits to the invariant mass and decay length distributions are provided in Figs. A.1–A.2 of Appendix A.

5   Systematic uncertainties

Systematic uncertainties are due to the measurement of the integrated luminosity (2.3%) [41], the determination of the signal yields, and the dimuon efficiencies and acceptances. Uncertainties in the estimation of the yields are evaluated by changing the signal and background models used in the maximum-likelihood fits. To assess the systematic uncertainty in the modeling of the signal invariant mass distribution of each state, the n and α parameters of the CB function are varied by up to ± 5 standard deviations, one at a time, while the mean, which is constrained in the nominal fit, is allowed to float. The half-differences between the largest resulting deviations of the signal yields measured in the fit from the nominal yields are added in quadrature to obtain an uncertainty in the modeling of the signal. The systematic uncertainty originating from a possibly imperfect description of the background is evaluated by changing the background model from an exponential to a linear function. The observed differences from the nominal signal yields are taken as a systematic uncertainty. The total uncertainty in the determination of the yields is obtained as the sum in quadrature of the uncertainties in signal and background, and is about 2.0% for all quarkonium states.

Uncertainties in the discrimination between charmonia that are promptly produced rather than originating from b hadron decays arise from the determination of the primary vertex position (the production point of the mesons, which enters in the calculation of the decay length) and from the modeling of the signal and background in the decay length distributions. We assess the uncertainty originating from the choice of the primary vertex by using an alternative to the average position of the luminous region, the position of the collision vertex closest to the dimuon vertex extrapolated towards the beam line. The systematic uncertainty related to the description of the background is evaluated by measuring the difference between the prompt fractions using the nominal fit and a fit modeling the background by the sum of four expo-

nential functions and a simplified resolution function composed of only one single Gaussian function. To study the impact of imperfect modeling of the resolution function, the scale parameters of the Gaussian functions that had Gaussian constraints in the nominal fit are varied by ± 1 standard deviation. Similarly, we assess the impact of modeling the nonprompt signal by fixing the parameterization of the exponential decay function. The systematic uncertainty stemming from the choice of the primary vertex is added in quadrature with the uncertainty derived from the fit strategy. The latter is calculated as half of the difference between the maximum deviations observed from the nominal fit when the above variations are applied one by one. The total systematic uncertainty in the determination of the nonprompt yield is less than 3% in almost all the (p_T, y) bins for the J/ψ meson, without a dominant contribution from any one of the sources described above. The largest systematic uncertainty in the $\psi(2S)$ measurements can reach a maximum of 16%, mostly owing to the uncertainty in the modeling of the background decay length distribution. The effect of pileup on the analysis results has been studied using both data and simulation, and found to be negligible.

Uncertainties in the single-muon efficiencies, reflecting their statistical precision as well as possible imperfections of the parametrization, are evaluated by varying the three parameters of the sigmoid function used to parameterize the single-muon efficiencies within their uncertainties. The resulting systematic uncertainties are nearly constant as a function of p_T and are around 2.5% for the J/ψ and $\psi(2S)$, and 1.8% for the Y(nS) in the central regions $|y| < 0.6$ and around 1% in the remaining rapidity regions. The L3 single-muon efficiencies are calculated from simulations because of the low number of collected events useful for their measurements. The corresponding uncertainty is estimated to be 3%.

Systematic uncertainties related to the ρ factor are of three kinds. The first originates from the number of events available in the control sample collected with the independent trigger used to evaluate the ρ factor. The relative uncertainty is about 1% from 20 to 50 GeV and increases to about 5% near 100 GeV, with no dependence on rapidity. The measurement of the ρ factor also requires the evaluation of an additional single-muon efficiency using the tag-and-probe method, which introduces an uncertainty of about 1% at low p_T (below 50 GeV) and up to 4% at high p_T. Moreover, we assign the fractional difference in the ρ factor obtained from data and simulation as a systematic uncertainty. The difference is in the range 2–5% up to 60 GeV and increases slowly for higher p_T, reaching a value of up to 15%, in the worst case. This is the dominant uncertainty for all the quarkonium states except the $\psi(2S)$.

The finite number of events generated for the acceptance calculation imposes a systematic uncertainty of 0.5% at low p_T and up to 6% at high p_T. Other sources of systematic uncertainties, like the kinematic modeling of simulated events, are found to have a negligible influence on the acceptance calculation. The effect of the quarkonium polarization on the acceptance is not treated as a systematic uncertainty; instead correction factors are provided in Appendix A to recalculate the cross sections according to different polarization scenarios.

For the cross sections measured in the rapidity-integrated range $|y| < 1.2$, we conservatively assign the total systematic uncertainties of the most-forward rapidity range, which are larger than the uncertainties for central rapidities. Taking advantage of the larger yields in the integrated-rapidity range, an additional p_T bin was added for each state. The systematic uncertainty in the yields for this bin was evaluated as described above for the other bins, while for other uncertainties the same value as in the neighboring lower-p_T bin was used. It was verified that systematic uncertainties extrapolated to the additional p_T bin have either negligible p_T dependence in that region or are negligibly small compared to other systematic or statistical uncertainties.

For the measurement of the ratios of the cross sections of the prompt $\psi(2S)$, $\Upsilon(2S)$, and $\Upsilon(3S)$ states relative to their ground states, the systematic uncertainties in the yields, the ρ factor, the single-muon efficiencies, and the acceptance are the only ones considered. Uncertainties in the yields for the ratio of $\psi(2S)$ and J/ψ cross sections are treated as uncorrelated, because their corresponding yields are determined from independent fits. In contrast, yield uncertainties are treated as correlated for the ratio of the $\Upsilon(nS)$ to $\Upsilon(1S)$ cross sections, as they are extracted from a combined fit to the three states, as shown in Fig. A.2 of Appendix A. The correlation factors are found to be negligible, and are on the order of 0.05. The same single-muon efficiencies are used for all the measured cross sections, therefore their uncertainties are treated as correlated in all the ratios. The systematic uncertainties in the ratios are determined by consistently varying the efficiencies in the numerator and the denominator by their uncertainties and recalculating the ratios. The resulting effect is less than 0.4%. The uncertainty in the integrated luminosity is fully correlated, and is not included in the ratios. Uncertainties in the ρ correction factor are treated as uncorrelated.

The statistical uncertainty in the $\psi(2S)$ to J/ψ cross section ratio is more important than any systematic uncertainty except for the high-p_T region, where the ρ factor uncertainty is the dominant one, reaching 28%. For the $\Upsilon(2S)$ to $\Upsilon(1S)$ and $\Upsilon(3S)$ to $\Upsilon(1S)$ cross section ratios, the uncertainty in the ρ factor dominates across the entire p_T region, ranging from 3% to 12%.

6   Results

The measured double-differential cross sections times the dimuon branching fractions are presented in Fig. 1 as a function of p_T, for four rapidity ranges in the case of the prompt J/ψ and $\psi(2S)$ states, and two rapidity ranges for the $\Upsilon(nS)$. The top panels of Fig. 2 show the measured cross sections times branching fractions for the rapidity-integrated range $|y| < 1.2$. The presented results are obtained under the assumption of unpolarized production, which is very close to the polarization that was measured by CMS [30, 31]. If the quarkonium states are fully polarized, the cross sections can change by up to 25%. The numerical values of the cross sections for all five quarkonium states in the chosen bins of p_T and $|y|$ in the unpolarized scenario are reported in Tables A.1–A.5 of Appendix A. Tables A.6–A.10 list the multiplicative scale factors needed to recalculate the cross sections in the three different polarization scenarios described in Section 3. The conversion to a new polarization scenario is achieved by multiplying the unpolarized cross section result in each (p_T, $|y|$) bin by the corresponding scale factor.

The NLO NRQCD predictions [42, 43] are in agreement with the measured cross sections times branching fractions within uncertainties, as shown in the top panels of Fig. 2. The ratios of the measured to predicted values are plotted in the middle panels of Fig. 2, where the vertical bars represent the experimental uncertainties. The shaded bands show the theoretical uncertainties stemming from the extraction of the LDMEs, renormalization scales, and the choice of c and b quark masses, added in quadrature with the uncertainties in the dimuon branching fractions [35]. The theory tends to underestimate (overestimate) the cross section for the J/ψ ($\psi(2S)$), while staying within the one-standard-deviation uncertainty band. The bottom panels of Fig. 2 show the ratios of the p_T differential cross sections times branching fractions measured at $\sqrt{s} = 13$ TeV and 7 TeV [25, 26] for $|y| < 1.2$. The 13 TeV cross sections of all five quarkonium states are factors of 1.5 to 3 larger than the corresponding 7 TeV cross sections, changing slowly as a function of dimuon p_T. An increase of this order is expected from the evolution of the parton distribution functions.

Figure 3 shows the production cross sections times dimuon branching fractions of the radial excitations relative to the ground state in the charmonium and bottomonium systems for $|y| <$
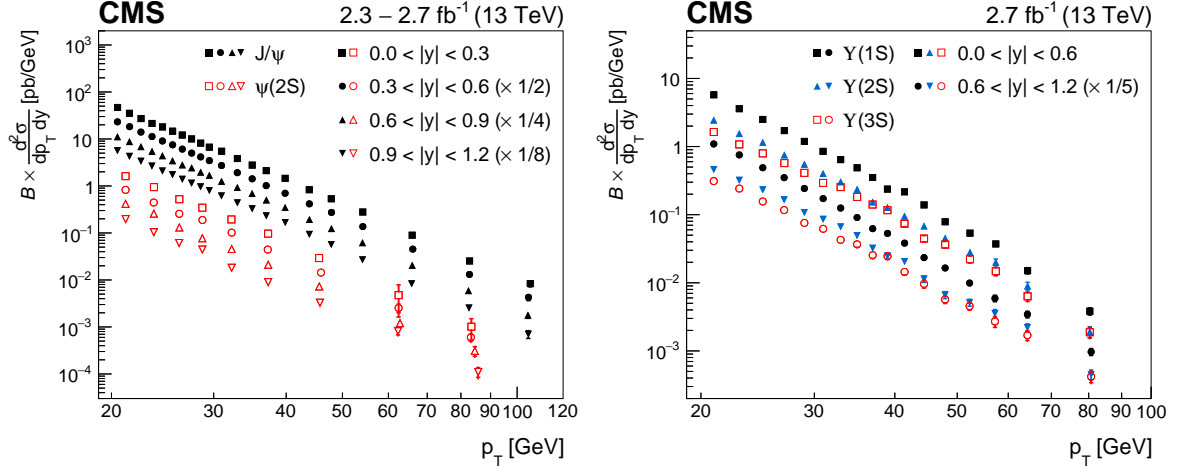
Figure 1: The product of the measured double-differential cross sections and the dimuon branching fractions for prompt J/ψ and $\psi(2S)$ (left) and the Y(nS) (right) mesons as a function of p_T, in four and two rapidity regions, respectively, assuming unpolarized dimuon decays. For presentation purposes, the individual points in the measurements are scaled by the factors given in the legends. The inner vertical bars on the data points represent the statistical uncertainty, while the outer bars show the statistical and systematic uncertainties, not including the 2.3% uncertainty in the integrated luminosity, added in quadrature. For most of the data points, the uncertainties are comparable to the size of the symbols.

1.2. The prompt $\psi(2S)$ to J/ψ meson cross section ratio is constant as a function of p_T, while the cross sections of the excited Y states relative to the Y(1S) show a slight increase with p_T. The numerical values of these ratios are reported in Table A.11 of Appendix A.

7 Summary

The double-differential production cross sections of the J/ψ, $\psi(2S)$, and Y(nS) (n = 1, 2, 3) quarkonium states have been measured, using their dimuon decay mode, in pp collisions at $\sqrt{s} = 13$ TeV with the CMS detector at the LHC. The production cross sections of all five S-wave states are presented in a single analysis. The measurement has been performed as a function of transverse momentum (p_T) in several bins of rapidity (y), covering a p_T range 20–120 GeV for the J/ψ meson and 20–100 GeV for the remaining states. The cross sections integrated over $|y| < 1.2$ are also presented, and extend the p_T reach to 150 and 130 GeV, respectively. Also presented are the ratios of cross sections measured at $\sqrt{s} = 13$ (this analysis) and 7 TeV (from Refs. [25, 26]), as well as the cross sections of the prompt $\psi(2S)$, Y(2S), and Y(3S) mesons relative to their ground states. These results will help in testing the underlying hypotheses of nonrelativistic quantum chromodynamics and in providing further input to constrain the theoretical parameters.
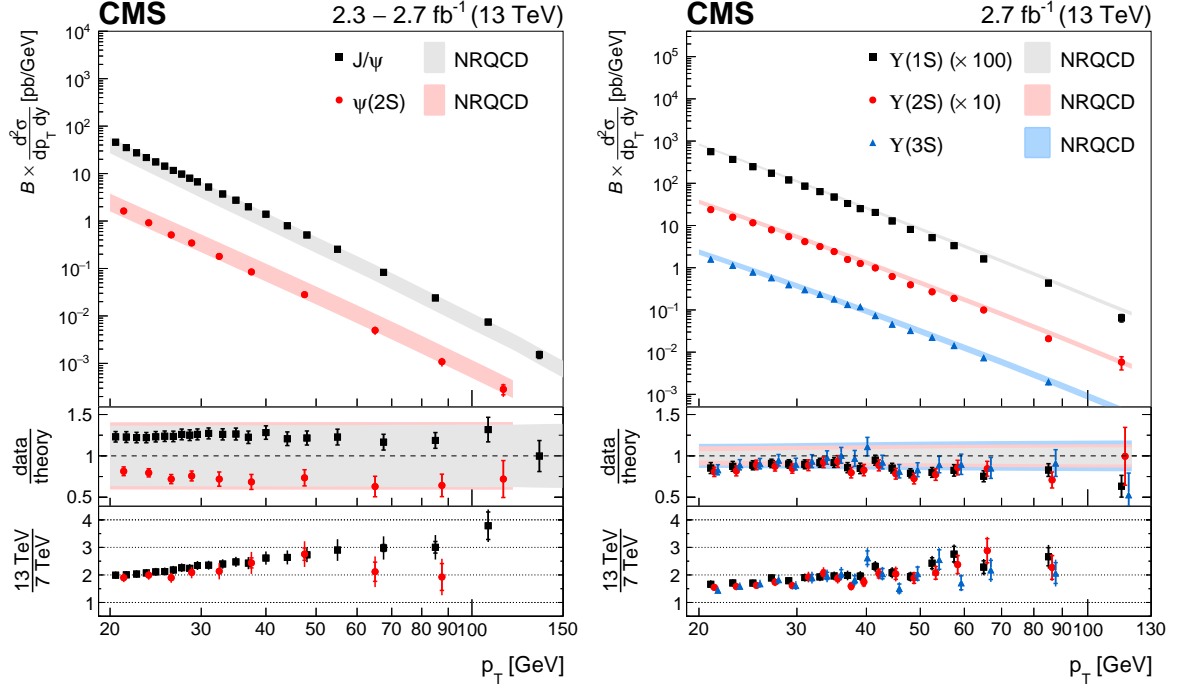
Figure 2: The measured double-differential cross sections times branching fractions of the prompt J/ψ and ψ(2S) (left) and the Y(nS) (right) mesons (markers), assuming unpolarized dimuon decays, as a function of p_T, for $|y| < 1.2$, compared to NLO NRQCD predictions [42, 43] (shaded bands). The inner vertical bars on the data points represent the statistical uncertainty, while the outer bars show the statistical and systematic uncertainties, including the integrated luminosity uncertainty of 2.3%, added in quadrature. The middle panels show the ratios of measurement to theory, where the vertical bars depict the total uncertainties in the measurement. The widths of the bands represent the theoretical uncertainty, added in quadrature with the uncertainties in the dimuon branching fractions [35]. The lower panels show the ratios of cross sections measured at $\sqrt{s} = 13$ TeV to those measured at 7 TeV [25, 26]. All uncertainties in the 7 and 13 TeV results are treated as uncorrelated.
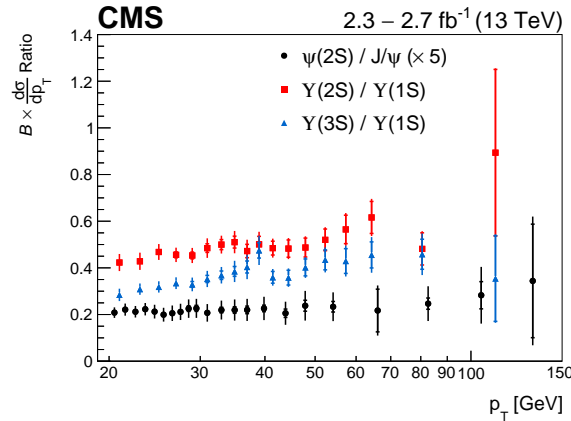
Figure 3: Ratios of the p_T differential cross sections times dimuon branching fractions of the prompt ψ(2S) to J/ψ, Y(2S) to Y(1S), and Y(3S) to Y(1S) mesons for $|y| < 1.2$. The inner vertical bars represent the statistical uncertainty, while the outer bars show the statistical and systematic uncertainties added in quadrature. The ratio of the ψ(2S) to J/ψ meson cross sections is multiplied by a factor 5 for better visibility.

Acknowledgments

References

[1] G. T. Bodwin, E. Braaten, and G. P. Lepage, "Rigorous QCD analysis of inclusive annihilation and production of heavy quarkonium", *Phys. Rev. D* **51** (1995) 1125, `doi:10.1103/PhysRevD.51.1125`. [Erratum: `doi:10.1103/PhysRevD.55.5853`].

[2] P. Cho and A. K. Leibovich, "Color-octet quarkonia production", *Phys. Rev. D* **53** (1996) 150, `doi:10.1103/PhysRevD.53.150`.

[3] P. Cho and A. K. Leibovich, "Color-octet quarkonia production. II", *Phys. Rev. D* **53** (1996) 6203, `doi:10.1103/PhysRevD.53.6203`.

[4] B. Gong, L.-P. Wan, J.-X. Wang, and H.-F. Zhang, "Complete next-to-leading-order study on the yield and polarization of Y(1S, 2S, 3S) at the Tevatron and LHC", *Phys. Rev. Lett.* **112** (2014) 032001, `doi:10.1103/PhysRevLett.112.032001`, `arXiv:1305.0748`.

[5] Z.-B. Kang, Y.-Q. Ma, J.-W. Qiu, and G. Sterman, "Heavy quarkonium production at collider energies: partonic cross section and polarization", *Phys. Rev. D* **91** (2015) 014030, `doi:10.1103/PhysRevD.91.014030`, `arXiv:1411.2456`.

[6] M. Butenschön and B. A. Kniehl, "J/ψ polarization at Tevatron and LHC: nonrelativistic-QCD factorization at the crossroads", *Phys. Rev. Lett.* **108** (2012) 172002, `doi:10.1103/PhysRevLett.108.172002`, `arXiv:1201.1872`.

[7] K.-T. Chao et al., "J/ψ polarization at hadron colliders in nonrelativistic QCD", *Phys. Rev. Lett.* **108** (2012) 242004, `doi:10.1103/PhysRevLett.108.242004`, `arXiv:1201.2675`.

[8] P. Faccioli et al., "Quarkonium production in the LHC era: a polarized perspective", *Phys. Lett. B* **736** (2014) 98, `doi:10.1016/j.physletb.2014.07.006`, `arXiv:1403.3970`.

[9] G. T. Bodwin, H. S. Chung, U.-R. Kim, and J. Lee, "Fragmentation contributions to J/ψ production at the Tevatron and the LHC", *Phys. Rev. Lett.* **113** (2014) 022001, `doi:10.1103/PhysRevLett.113.022001`, `arXiv:1403.3612`.

[10] LHCb Collaboration, "Measurement of the cross-section ratio $\sigma(\chi_{c2})/\sigma(\chi_{c1})$ for prompt χ_c production at $\sqrt{s} = 7$ TeV", *Phys. Lett. B* **714** (2012) 215, `doi:10.1016/j.physletb.2012.06.077`, `arXiv:1202.1080`.

[11] LHCb Collaboration, "Measurement of the $\chi_b(3P)$ mass and of the relative rate of $\chi_{b1}(1P)$ and $\chi_{b2}(1P)$ production", *JHEP* **10** (2014) 88, `doi:10.1007/JHEP10(2014)088`, `arXiv:1409.1408`.

[12] ATLAS Collaboration, "Measurement of χ_{c1} and χ_{c2} production with $\sqrt{s} = 7$ TeV pp collisions at ATLAS", *JHEP* **07** (2014) 154, `doi:10.1007/JHEP07(2014)154`, `arXiv:1404.7035`.

[13] CMS Collaboration, "Measurement of the production cross section ratio $\sigma(\chi_{b2}(1P))/\sigma(\chi_{b1}(1P))$ in pp collisions at $\sqrt{s} = 8$ TeV", *Phys. Lett. B* **743** (2015) 383, `doi:10.1016/j.physletb.2015.02.048`, `arXiv:1409.5761`.

[14] CMS Collaboration, "Measurement of the relative prompt production rate of χ_{c2} and χ_{c1} in pp collisions at $\sqrt{s} = 7$ TeV", *Eur. Phys. J. C* **72** (2012) 2251, `doi:10.1140/epjc/s10052-012-2251-3`, `arXiv:1210.0875`.

[15] LHCb Collaboration, "Measurement of the $\eta_c(1S)$ production cross-section in proton-proton collisions via the decay $\eta_c(1S) \to p\overline{p}$", *Eur. Phys. J. C* **75** (2015) 311, `doi:10.1140/epjc/s10052-015-3502-x`, `arXiv:1409.3612`.

[16] ATLAS Collaboration, "Measurement of the differential cross-sections of inclusive, prompt and non-prompt J/ψ production in proton-proton collisions at $\sqrt{s} = 7$ TeV", *Nucl. Phys. B* **850** (2011) 387, `doi:10.1016/j.nuclphysb.2011.05.015`, `arXiv:1104.3038`.

[17] ATLAS Collaboration, "Measurement of the production cross-section of $\psi(2S) \to J/\psi(\to \mu^+\mu^-)\pi^+\pi^-$ in pp collisions at $\sqrt{s} = 7$ TeV at ATLAS", *JHEP* **09** (2014) 079, `doi:10.1007/JHEP09(2014)079`, `arXiv:1407.5532`.

[18] ATLAS Collaboration, "Measurement of Upsilon production in 7 TeV pp collisions at ATLAS", *Phys. Rev. D* **87** (2013) 052004, `doi:10.1103/PhysRevD.87.052004`, `arXiv:1211.7255`.

[19] LHCb Collaboration, "Measurement of J/ψ production in pp collisions at $\sqrt{s} = 7$ TeV", *Eur. Phys. J. C* **71** (2011) 1645, `doi:10.1140/epjc/s10052-011-1645-y`, `arXiv:1103.0423`.

[20] LHCb Collaboration, "Measurement of $\psi(2S)$ meson production in pp collisions at $\sqrt{s} = 7$ TeV", *Eur. Phys. J. C* **72** (2012) 2100, `doi:10.1140/epjc/s10052-012-2100-4`, `arXiv:1204.1258`.

[21] LHCb Collaboration, "Measurement of Upsilon production in pp collisions at $\sqrt{s} = 7$ TeV", *Eur. Phys. J. C* **72** (2012) 2025, `doi:10.1140/epjc/s10052-012-2025-y`, `arXiv:1202.6579`.

[22] ALICE Collaboration, "Measurement of prompt J/ψ and beauty hadron production cross sections at mid-rapidity in pp collisions at $\sqrt{s} = 7$ TeV", *JHEP* **11** (2012) 065, `doi:10.1007/JHEP11(2012)065`, `arXiv:1205.5880`.

[23] CMS Collaboration, "Measurement of the inclusive Y production cross section in pp collisions at $\sqrt{s} = 7$ TeV", *Phys. Rev. D* **83** (2011) 112004, `doi:10.1103/PhysRevD.83.112004`, `arXiv:1012.5545`.

[24] CMS Collaboration, "Measurement of the Y(1S), Y(2S), and Y(3S) cross sections in pp collisions at $\sqrt{s} = 7$ TeV", *Phys. Lett. B* **727** (2013) 101, `doi:10.1016/j.physletb.2013.10.033`, `arXiv:1303.5900`.

[25] CMS Collaboration, "Measurement of J/ψ and $\psi(2S)$ prompt double-differential cross sections in pp collisions at $\sqrt{s} = 7$ TeV", *Phys. Rev. Lett.* **114** (2015) 191802, `doi:10.1103/PhysRevLett.114.191802`, `arXiv:1502.04155`.

[26] CMS Collaboration, "Measurements of the Y(1S), Y(2S), and Y(3S) differential cross sections in pp collisions at $\sqrt{s} = 7$ TeV", *Phys. Lett. B* **749** (2015) 14, `doi:10.1016/j.physletb.2015.07.037`, `arXiv:1501.07750`.

[27] CMS Collaboration, "Suppression of non-prompt J/ψ, prompt J/ψ, and Y(1S) in PbPb collisions at $\sqrt{s_{NN}} = 2.76$ TeV", *Journal of High Energy Physics* **5** (2012) 63, `doi:10.1007/JHEP05(2012)063`.

[28] CMS Collaboration, "Suppression of Y(1S), Y(2S)and Y(3S) production in PbPb collisions at $\sqrt{s_{NN}} = 2.76$ TeV", *Phys. Lett. B* **770** (2017) 357, `doi:10.1016/j.physletb.2017.04.031`, `arXiv:1611.01510`.

[29] ALICE Collaboration, "J/ψ polarization in pp collisions at $\sqrt{s} = 7$ TeV", *Phys. Rev. Lett.* **108** (2012) 082001, `doi:10.1103/PhysRevLett.108.082001`, `arXiv:1111.1630`.

[30] CMS Collaboration, "Measurement of the prompt J/ψ and $\psi(2S)$ polarizations in pp collisions at $\sqrt{s} = 7$ TeV", *Phys. Lett. B* **727** (2013) 381, `doi:10.1016/j.physletb.2013.10.055`, `arXiv:1307.6070`.

[31] CMS Collaboration, "Measurement of the Υ(1S), Υ(2S), and Υ(3S) polarizations in pp collisions at $\sqrt{s} = 7$ TeV", *Phys. Rev. Lett.* **110** (2013) 081802, `doi:10.1103/PhysRevLett.110.081802, arXiv:1209.2922`.

[32] LHCb Collaboration, "Measurement of J/ψ polarization in pp collisions at $\sqrt{s} = 7$ TeV", *Eur. Phys. J. C* **73** (2013) 2631, `doi:10.1140/epjc/s10052-013-2631-3, arXiv:1307.6379`.

[33] LHCb Collaboration, "Measurement of $\psi(2S)$ polarisation in pp collisions at $\sqrt{s} = 7$ TeV", *Eur. Phys. J. C* **74** (2014) 2872, `doi:10.1140/epjc/s10052-014-2872-9, arXiv:1403.1339`.

[34] CMS Collaboration, "Prompt and non-prompt J/ψ production in pp collisions at $\sqrt{s} = 7$ TeV", *Eur. Phys. J. C* **71** (2011) 1575, `doi:10.1140/epjc/s10052-011-1575-8, arXiv:1011.4193`.

[35] Particle Data Group, C. Patrignani et al., "Review of Particle Physics", *Chin. Phys. C* **40** (2016) 100001, `doi:10.1088/1674-1137/40/10/100001`.

[36] CMS Collaboration, "Performance of CMS muon reconstruction in pp collision events at $\sqrt{s} = 7$ TeV", *JINST* **7** (2012) P10002, `doi:10.1088/1748-0221/7/10/P10002, arXiv:1206.4071`.

[37] CMS Collaboration, "The CMS experiment at the CERN LHC", *JINST* **3** (2008) S08004, `doi:10.1088/1748-0221/3/08/S08004`.

[38] CMS Collaboration, "The CMS trigger system", *JINST* **12** (2017) P01020, `doi:10.1088/1748-0221/12/01/P01020, arXiv:1609.02366`.

[39] T. Sjöstrand, S. Mrenna, and P. Skands, "A brief introduction to PYTHIA 8.1", *Comp. Phys. Comm.* **178** (2008) 852, `doi:10.1016/j.cpc.2008.01.036, arXiv:0710.3820`.

[40] M. J. Oreglia, "A study of the reactions $\psi' \to \gamma\gamma\psi$". PhD thesis, Stanford University, 1980. SLAC Report SLAC-R-236, see Appendix D.

[41] CMS Collaboration, "Preliminary CMS luminosity measurement for the 2015 data taking period", CMS Physics Analysis Summary CMS-PAS-LUM-15-001, 2017.

[42] Y.-Q. Ma, K. Wang, and K.-T. Chao, "J/ψ (ψ') production at the Tevatron and LHC at $\mathcal{O}(\alpha_s^4 v^4)$ in nonrelativistic QCD", *Phys. Rev. Lett.* **106** (2011) 042002, `doi:10.1103/PhysRevLett.106.042002, arXiv:1009.3655`.

[43] H. Han et al., "Υ(nS) and χ_b(nP) production at hadron colliders in nonrelativistic QCD", *Phys. Rev. D* **94** (2016) 014028, `doi:10.1103/PhysRevD.94.014028, arXiv:1410.8537`.

A   Dimuon invariant mass and lifetime distributions, numerical values of differential cross section, and correction factors for alternative polarization scenarios
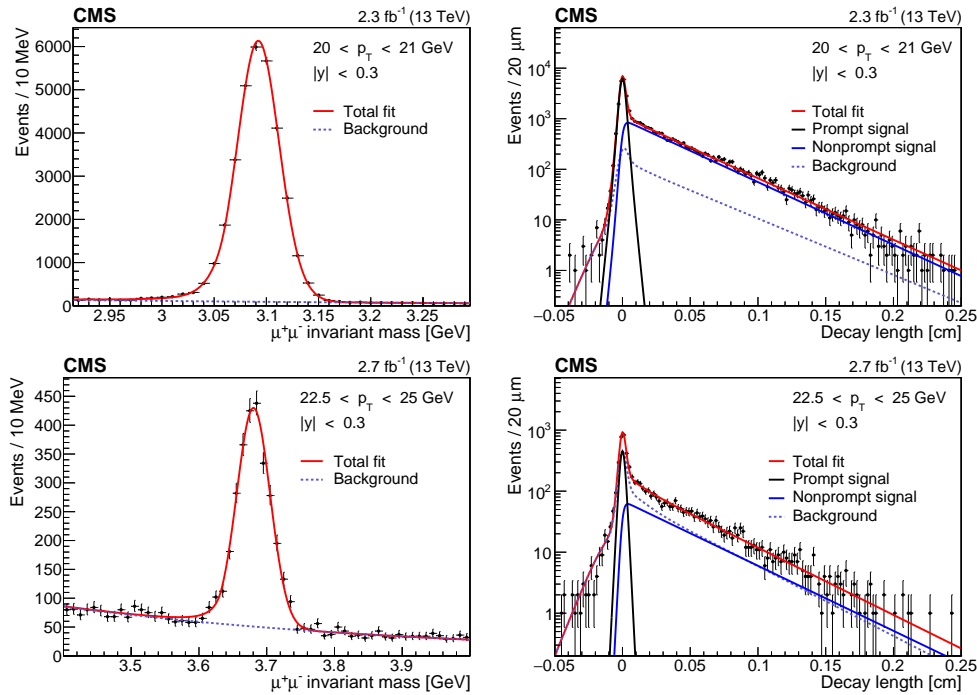
Figure A.1: Examples of fits of the dimuon invariant mass (left) and decay length (right) distributions for J/ψ (upper row) and $\psi(2S)$ (lower row) candidate events in the p_T and $|y|$ ranges given in the plots. The results from the total fit and from the various components included in the fit are shown.
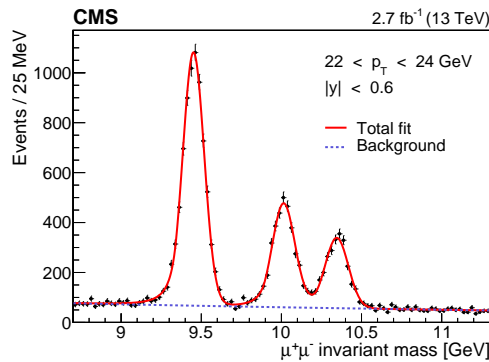
Figure A.2: Examples of a fit of the dimuon invariant mass distribution for the $Y(nS)$ candidate events in the p_T and $|y|$ ranges given in the plot. The results from the total fit and for the background component are shown.

Table A.1: Double-differential cross section times the dimuon branching fraction of the J/ψ meson for different ranges of p_T, in bins of $|y|$ and for the full $|y|$ range, for the unpolarized decay hypothesis, with their statistical and systematic uncertainties in percent. The average p_T value in each bin is also given. The global uncertainty in the integrated luminosity of 2.3% is not included in the systematic uncertainties.

$$B\, \mathrm{d}\sigma^2/\mathrm{d}p_T\mathrm{d}y$$

p_T [GeV]	$\langle p_T \rangle$ [GeV]	$|y| < 0.3$ [pb/GeV]	stat %	syst %	$0.3 < |y| < 0.6$ [pb/GeV]	stat %	syst %	$0.6 < |y| < 0.9$ [pb/GeV]	stat %	syst %	$0.9 < |y| < 1.2$ [pb/GeV]	stat %	syst %	$|y| < 1.2$ [pb/GeV]	stat %	syst %
20–21	20.5	4.68E+01	1.7	5.3	4.63E+01	1.3	4.6	4.47E+01	1.2	4.5	4.51E+01	1.3	4.6	4.58E+01	0.7	4.6
21–22	21.5	3.52E+01	1.3	5.4	3.65E+01	1.2	4.8	3.52E+01	1.2	4.6	3.42E+01	1.3	4.8	3.53E+01	0.6	4.8
22–23	22.5	2.72E+01	1.4	5.2	2.80E+01	1.3	4.5	2.75E+01	1.3	4.4	2.69E+01	1.3	4.6	2.74E+01	0.7	4.6
23–24	23.5	2.14E+01	1.5	5.0	2.25E+01	1.4	4.5	2.18E+01	1.4	4.3	2.12E+01	1.5	4.4	2.18E+01	0.7	4.5
24–25	24.5	1.80E+01	1.6	5.0	1.81E+01	1.5	4.5	1.76E+01	1.5	4.3	1.66E+01	1.6	4.5	1.76E+01	0.8	4.5
25–26	25.5	1.46E+01	1.8	5.0	1.50E+01	1.7	4.5	1.38E+01	1.7	4.3	1.39E+01	1.8	4.5	1.43E+01	0.9	4.5
26–27	26.5	1.21E+01	1.9	5.1	1.22E+01	1.8	4.4	1.11E+01	1.9	4.3	1.11E+01	1.9	4.5	1.17E+01	0.9	4.5
27–28	27.5	1.00E+01	2.1	5.0	1.00E+01	2.0	4.4	9.17E+00	2.0	4.3	9.17E+00	2.1	4.5	9.75E+00	1.0	4.5
28–29	28.5	8.14E+00	2.3	5.1	8.31E+00	2.2	4.5	7.67E+00	2.2	4.3	7.67E+00	2.3	4.5	7.99E+00	1.1	4.5
29–30	29.5	6.68E+00	2.5	5.2	6.92E+00	2.4	4.5	6.78E+00	2.4	4.4	6.39E+00	2.5	4.6	6.70E+00	1.2	4.5
30–32	31.0	5.47E+00	1.9	5.2	5.44E+00	1.9	4.5	5.03E+00	1.9	4.5	4.91E+00	2.0	4.6	5.20E+00	1.0	4.6
32–34	33.0	3.84E+00	2.3	5.4	3.84E+00	2.2	4.6	3.72E+00	2.2	4.4	3.50E+00	2.3	4.8	3.72E+00	1.1	4.7
34–36	35.0	2.78E+00	2.7	5.7	2.84E+00	2.5	4.9	2.76E+00	2.5	4.9	2.62E+00	2.7	5.1	2.75E+00	1.3	5.0
36–38	37.0	2.12E+00	3.1	6.2	2.03E+00	2.9	5.4	2.02E+00	3.0	5.3	1.85E+00	3.1	5.6	2.00E+00	1.5	5.5
38–42	39.8	1.45E+00	2.6	6.4	1.40E+00	2.5	5.7	1.39E+00	2.5	5.6	1.33E+00	2.6	5.9	1.39E+00	1.3	5.8
42–46	43.8	8.33E-01	3.3	6.9	8.33E-01	3.2	6.1	7.74E-01	3.3	5.9	7.47E-01	3.4	6.5	7.96E-01	1.7	6.2
46–50	47.8	5.34E-01	4.2	7.0	5.48E-01	4.0	6.1	4.96E-01	4.2	6.1	4.54E-01	4.5	6.7	5.08E-01	2.1	6.3
50–60	54.2	2.79E-01	3.7	7.8	2.74E-01	3.5	7.1	2.49E-01	3.7	7.1	2.14E-01	4.1	7.7	2.54E-01	1.9	7.2
60–75	66.0	8.96E-02	5.4	8.0	9.05E-02	5.0	6.9	8.23E-02	5.6	6.9	6.64E-02	6.2	8.2	8.28E-02	2.7	7.3
75–95	82.7	2.54E-02	9.0	7.7	2.62E-02	8.5	6.4	2.37E-02	8.7	6.4	2.03E-02	9.6	7.6	2.39E-02	4.4	6.3
95–120	104.7	8.37E-03	15	8.3	8.56E-03	15	8.2	7.16E-03	15	7.3	5.61E-03	19	9.1	7.42E-03	7.7	7.9
120–150	131.1													1.53E-03	17	7.9

Table A.2: Double-differential cross section times the dimuon branching fraction of the $\psi(2S)$ meson for different ranges of p_T, in bins of $|y|$ and for the full $|y|$ range, for the unpolarized decay hypothesis, with their statistical and systematic uncertainties in percent. The average p_T value in each bin is also given. The global uncertainty in the integrated luminosity of 2.3% is not included in the systematic uncertainties.

$$\mathcal{B}\,\mathrm{d}\sigma^2/\mathrm{d}p_T\mathrm{d}y$$

p_T [GeV]	$\langle p_T \rangle$ [GeV]	$|y| < 0.3$			$0.3 < |y| < 0.6$			$0.6 < |y| < 0.9$			$0.9 < |y| < 1.2$			$|y| < 1.2$		
		[pb/GeV]	stat %	syst %	[pb/GeV]	stat %	syst %	[pb/GeV]	stat %	syst %	[pb/GeV]	stat %	syst %	[pb/GeV]	stat %	syst %
20–22	21.1	1.62E+00	3.3	5.4	1.65E+00	3.3	5.5	1.67E+00	3.2	5.0	1.58E+00	3.6	5.8	1.63E+00	1.6	5.8
22–25	23.7	9.46E-01	4.2	5.0	8.90E-01	4.4	5.0	1.03E+00	3.9	4.6	8.30E-01	4.8	5.3	9.19E-01	2.1	5.4
25–28	26.2	5.23E-01	5.6	5.0	5.12E-01	5.7	5.2	5.23E-01	5.3	4.4	4.89E-01	6.1	6.7	5.10E-01	2.8	6.8
28–30	28.7	3.45E-01	6.9	5.4	3.77E-01	6.3	5.6	3.08E-01	7.3	5.0	3.55E-01	6.8	6.7	3.45E-01	3.3	6.8
30–35	32.2	1.94E-01	6.4	6.1	2.04E-01	6.2	7.0	1.82E-01	6.6	6.2	1.46E-01	8.2	11	1.80E-01	3.3	11
35–40	37.2	9.68E-02	9.2	7.3	8.87E-02	9.1	8.1	8.42E-02	9.2	9.0	7.22E-02	11	12	8.46E-02	4.7	12
40–55	45.7	2.93E-02	9.3	7.5	2.87E-02	9.4	8.2	2.90E-02	9.6	9.1	2.63E-02	11	12	2.81E-02	4.8	12
55–75	62.5	4.75E-03	66	12	5.07E-03	21	15	4.82E-03	10	15	6.59E-03	18	17	4.97E-03	11	16
75–100	84.2	1.01E-03	48	18	1.20E-03	17	17	1.24E-03	23	18	8.81E-04	23	20	1.08E-03	6.6	20
100–130	111.0													2.85E-04	24	20

Table A.3: Double-differential cross section times the dimuon branching fraction of the Υ(1S) meson for different ranges of p_T, in bins of $|y|$ and for the full $|y|$ range, for the unpolarized decay hypothesis, with their statistical and systematic uncertainties in percent. The average p_T value in each bin is also given. The global uncertainty in the integrated luminosity of 2.3% is not included in the systematic uncertainties.

p_T [GeV]	$\langle p_T \rangle$ [GeV]	$B\, d\sigma^2/dp_T dy$								
		$|y| < 0.6$			$0.6 < |y| < 1.2$			$|y| < 1.2$		
		[pb/GeV]	stat %	syst %	[pb/GeV]	stat %	syst %	[pb/GeV]	stat %	syst %
20–22	20.9	5.76E+00	1.7	7.1	5.46E+00	1.7	7.8	5.62E+00	0.9	7.3
22–24	22.9	3.60E+00	1.6	6.0	3.77E+00	2.1	6.7	3.68E+00	1.1	6.3
24–26	25.0	2.50E+00	1.9	5.3	2.44E+00	2.1	6.1	2.47E+00	1.3	5.6
26–28	26.9	1.72E+00	2.2	4.8	1.75E+00	2.5	5.3	1.73E+00	1.5	4.9
28–30	29.0	1.19E+00	2.6	4.9	1.21E+00	3.1	5.2	1.20E+00	1.8	4.9
30–32	31.0	8.50E-01	3.5	4.9	8.62E-01	3.5	5.3	8.55E-01	2.1	5.1
32–34	33.0	6.43E-01	4.0	4.9	6.26E-01	4.1	5.0	6.36E-01	2.4	4.8
34–36	35.0	4.88E-01	4.2	4.7	4.55E-01	5.1	5.4	4.72E-01	2.8	5.3
36–38	37.0	3.52E-01	5.2	4.8	3.12E-01	6.0	6.1	3.32E-01	3.4	5.8
38–40	39.0	2.37E-01	6.1	5.0	2.65E-01	6.5	6.2	2.51E-01	3.9	6.0
40–43	41.4	2.17E-01	5.4	5.4	1.91E-01	5.7	5.1	2.04E-01	3.5	4.8
43–46	44.4	1.39E-01	6.0	5.5	1.17E-01	7.3	5.0	1.28E-01	4.3	4.9
46–50	47.9	7.87E-02	7.0	5.2	8.25E-02	7.0	5.1	8.07E-02	4.6	4.6
50–55	52.3	5.36E-02	7.4	5.0	4.96E-02	8.2	5.2	5.16E-02	5.2	4.7
55–60	57.3	3.72E-02	8.8	5.4	2.96E-02	11	5.6	3.33E-02	6.5	4.8
60–70	64.3	1.51E-02	10	5.2	1.72E-02	11	5.6	1.62E-02	6.8	5.1
70–100	80.5	3.83E-03	12	5.4	4.85E-03	12	5.6	4.32E-03	7.7	4.7
100–130	111.5							6.48E-04	20	4.7

Table A.4: Double-differential cross section times the dimuon branching fraction of the Υ(2S) meson for different ranges of p_T, in bins of $|y|$ and for the full $|y|$ range, for the unpolarized decay hypothesis, with their statistical and systematic uncertainties in percent. The average p_T value in each bin is also given. The global uncertainty in the integrated luminosity of 2.3% is not included in the systematic uncertainties.

p_T [GeV]	$\langle p_T \rangle$ [GeV]	$\mathcal{B}\,\mathrm{d}\sigma^2/\mathrm{d}p_T\mathrm{d}y$								
		$|y| < 0.6$			$0.6 < |y| < 1.2$			$|y| < 1.2$		
		[pb/GeV]	stat %	syst %	[pb/GeV]	stat %	syst %	[pb/GeV]	stat %	syst %
20–22	20.9	2.45E+00	2.6	6.1	2.30E+00	2.7	6.9	2.38E+00	1.4	6.4
22–24	22.9	1.55E+00	2.3	5.7	1.60E+00	3.3	7.1	1.57E+00	1.7	6.8
24–26	25.0	1.15E+00	2.7	5.2	1.16E+00	3.1	6.1	1.16E+00	1.9	5.8
26–28	26.9	7.54E-01	3.3	4.9	8.27E-01	3.7	5.9	7.89E-01	2.3	5.6
28–30	29.0	5.51E-01	3.7	5.0	5.39E-01	4.6	5.8	5.45E-01	2.7	5.5
30–32	31.0	4.02E-01	4.8	5.4	4.28E-01	5.2	6.5	4.14E-01	3.1	6.3
32–34	33.0	3.04E-01	5.8	6.0	3.31E-01	5.8	5.7	3.18E-01	3.6	5.5
34–36	35.0	2.36E-01	5.9	4.8	2.47E-01	7.6	6.2	2.41E-01	4.1	6.0
36–38	37.0	1.54E-01	7.2	4.7	1.61E-01	8.3	6.0	1.57E-01	5.0	5.6
38–40	39.0	1.28E-01	7.8	4.9	1.23E-01	9.4	5.8	1.26E-01	5.7	5.6
40–43	41.4	9.52E-02	7.6	5.2	1.03E-01	8.0	5.4	9.89E-02	5.0	5.1
43–46	44.4	6.83E-02	8.3	4.9	5.68E-02	11	5.0	6.19E-02	6.4	4.7
46–50	47.9	4.53E-02	9.1	4.8	3.32E-02	12	5.4	3.93E-02	6.9	5.0
50–55	52.3	2.81E-02	9.9	5.1	2.57E-02	12	5.4	2.68E-02	7.3	4.9
55–60	57.3	2.00E-02	11	5.5	1.77E-02	14	5.8	1.88E-02	8.6	5.1
60–70	64.3	8.99E-03	13	5.5	1.10E-02	13	6.3	9.96E-03	8.8	5.5
70–100	80.5	1.91E-03	19	6.3	2.24E-03	17	7.1	2.08E-03	12	5.9
100–130	111.5							5.79E-04	35	6.0

Table A.5: Double-differential cross section times the dimuon branching fraction of the $\Upsilon(3S)$ meson for different ranges of $|y|$, in bins of $|y|$ and for the full $|y|$ range, for the unpolarized decay hypothesis, with their statistical and systematic uncertainties in percent. The average p_T value in each bin is also given. The global uncertainty in the integrated luminosity of 2.3% is not included in the systematic uncertainties.

p_T [GeV]	$\langle p_T \rangle$ [GeV]	$|y| < 0.6$ [pb/GeV]	stat %	syst %	$0.6 < |y| < 1.2$ [pb/GeV]	stat %	syst %	$|y| < 1.2$ [pb/GeV]	stat %	syst %
					$B\,\mathrm{d}\sigma^2/\mathrm{d}p_T\mathrm{d}y$					
20–22	20.9	1.64E+00	3.3	7.3	1.55E+00	3.5	7.1	1.60E+00	1.8	6.7
22–24	22.9	1.08E+00	2.9	6.0	1.21E+00	4.0	6.5	1.13E+00	2.0	6.2
24–26	25.0	7.94E-01	3.4	6.2	7.81E-01	4.1	6.4	7.88E-01	2.4	6.1
26–28	26.9	5.72E-01	3.9	6.2	5.84E-01	4.8	6.6	5.79E-01	2.8	6.3
28–30	29.0	4.11E-01	4.5	5.8	3.79E-01	6.0	7.0	3.96E-01	3.3	6.8
30–32	31.0	2.93E-01	6.0	6.4	3.10E-01	6.6	7.3	3.01E-01	3.8	7.0
32–34	33.0	2.54E-01	6.9	6.1	2.13E-01	7.9	6.9	2.34E-01	4.3	6.8
34–36	35.0	1.82E-01	7.0	5.9	1.84E-01	9.7	8.1	1.82E-01	4.7	7.9
36–38	37.0	1.41E-01	7.9	5.8	1.27E-01	10	8.2	1.34E-01	5.4	8.0
38–40	39.0	1.16E-01	8.7	6.0	1.23E-01	11	8.0	1.19E-01	5.7	7.9
40–43	41.4	7.36E-02	9.4	6.4	7.23E-02	10	6.5	7.33E-02	6.1	6.1
43–46	44.4	4.46E-02	11	6.3	4.81E-02	13	6.0	4.59E-02	7.7	5.8
46–50	47.9	3.64E-02	11	6.8	2.84E-02	13	6.4	3.24E-02	7.7	6.0
50–55	52.3	2.22E-02	12	6.9	2.28E-02	13	7.2	2.24E-02	8.4	6.9
55–60	57.3	1.48E-02	14	8.1	1.35E-02	18	8.8	1.43E-02	11	8.3
60–70	64.3	6.34E-03	16	10	8.50E-03	17	11	7.36E-03	10	10
70–100	80.5	1.88E-03	17	13	2.10E-03	19	13	1.98E-03	12	13
100–130	111.5							2.30E-04	48	13

Table A.6: Multiplicative scaling factors to obtain the J/ψ differential cross sections for different polarization scenarios ($\lambda_\theta^{\mathrm{HX}} = +1, k, -1$) from the unpolarized cross section measurements given in Table A.1. The value of k is taken equal to $+0.10$, and corresponds to an average over p_T of the CMS measurement [30].

p_T [GeV]	$|y| < 0.3$			$0.3 < |y| < 0.6$			$0.6 < |y| < 0.9$			$0.9 < |y| < 1.2$			$|y| < 1.2$		
	$\lambda_\theta{=}{+}1$	$\lambda_\theta{=}k$	$\lambda_\theta{=}{-}1$	$\lambda_\theta{=}{+}1$	$\lambda_\theta{=}k$	$\lambda_\theta{=}{-}1$	$\lambda_\theta{=}{+}1$	$\lambda_\theta{=}k$	$\lambda_\theta{=}{-}1$	$\lambda_\theta{=}{+}1$	$\lambda_\theta{=}k$	$\lambda_\theta{=}{-}1$	$\lambda_\theta{=}{+}1$	$\lambda_\theta{=}k$	$\lambda_\theta{=}{-}1$
20–21	1.20	1.02	0.75	1.17	1.01	0.75	1.18	1.02	0.76	1.18	1.02	0.76	1.19	1.02	0.76
21–22	1.19	1.02	0.76	1.17	1.01	0.76	1.18	1.02	0.77	1.17	1.02	0.77	1.18	1.02	0.76
22–23	1.19	1.02	0.76	1.16	1.01	0.77	1.17	1.02	0.78	1.17	1.02	0.78	1.17	1.02	0.77
23–24	1.18	1.02	0.77	1.16	1.01	0.77	1.16	1.02	0.78	1.16	1.02	0.78	1.16	1.02	0.78
24–25	1.17	1.02	0.77	1.15	1.01	0.78	1.16	1.02	0.79	1.15	1.02	0.79	1.16	1.02	0.78
25–26	1.17	1.02	0.78	1.15	1.01	0.78	1.15	1.02	0.79	1.15	1.02	0.79	1.15	1.02	0.79
26–27	1.16	1.02	0.78	1.14	1.01	0.79	1.15	1.02	0.79	1.14	1.02	0.80	1.15	1.02	0.79
27–28	1.16	1.02	0.79	1.14	1.01	0.79	1.14	1.02	0.80	1.14	1.02	0.81	1.14	1.02	0.80
28–29	1.15	1.02	0.79	1.13	1.01	0.80	1.13	1.02	0.81	1.14	1.02	0.81	1.14	1.01	0.80
29–30	1.14	1.02	0.80	1.13	1.01	0.80	1.13	1.02	0.81	1.13	1.02	0.81	1.13	1.01	0.81
30–32	1.14	1.02	0.81	1.12	1.01	0.81	1.12	1.01	0.82	1.13	1.01	0.82	1.13	1.01	0.81
32–34	1.13	1.02	0.82	1.11	1.01	0.82	1.12	1.01	0.82	1.12	1.01	0.82	1.12	1.01	0.82
34–36	1.13	1.02	0.82	1.11	1.01	0.82	1.11	1.01	0.83	1.12	1.01	0.83	1.12	1.01	0.83
36–38	1.11	1.01	0.83	1.11	1.01	0.83	1.11	1.01	0.84	1.11	1.01	0.85	1.11	1.01	0.84
38–42	1.11	1.01	0.84	1.10	1.01	0.84	1.10	1.01	0.85	1.10	1.01	0.85	1.10	1.01	0.84
42–46	1.10	1.01	0.85	1.09	1.01	0.85	1.09	1.01	0.86	1.09	1.01	0.85	1.09	1.01	0.85
46–50	1.09	1.01	0.86	1.08	1.01	0.86	1.08	1.01	0.87	1.09	1.01	0.86	1.09	1.01	0.86
50–60	1.08	1.01	0.88	1.06	1.01	0.89	1.07	1.01	0.88	1.08	1.01	0.88	1.07	1.01	0.88
60–75	1.06	1.01	0.89	1.05	1.00	0.90	1.06	1.01	0.90	1.06	1.01	0.90	1.06	1.01	0.90
75–95	1.05	1.01	0.91	1.04	1.00	0.93	1.04	1.01	0.92	1.05	1.01	0.91	1.04	1.01	0.92
95–120	1.03	1.01	0.93	1.02	1.00	0.94	1.03	1.00	0.94	1.04	1.01	0.92	1.03	1.00	0.93
120–150													1.03	1.00	0.93

Table A.7: Multiplicative scaling factors to obtain the $\psi(2S)$ differential cross sections for different polarization scenarios ($\lambda_\theta^{\mathrm{HX}} = +1, k, -1$) from the unpolarized cross section measurements given in Table A.1. The value of k is taken equal to $+0.03$, and corresponds to an average over p_{T} of the CMS measurement [30].

p_{T} [GeV]	$|y| < 0.3$			$0.3 < |y| < 0.6$			$0.6 < |y| < 0.9$			$0.9 < |y| < 1.2$			$|y| < 1.2$		
	$\lambda_\theta{=}{+}1$	$\lambda_\theta{=}k$	$\lambda_\theta{=}{-}1$	$\lambda_\theta{=}{+}1$	$\lambda_\theta{=}k$	$\lambda_\theta{=}{-}1$	$\lambda_\theta{=}{+}1$	$\lambda_\theta{=}k$	$\lambda_\theta{=}{-}1$	$\lambda_\theta{=}{+}1$	$\lambda_\theta{=}k$	$\lambda_\theta{=}{-}1$	$\lambda_\theta{=}{+}1$	$\lambda_\theta{=}k$	$\lambda_\theta{=}{-}1$
20–22	1.19	1.01	0.76	1.17	0.99	0.75	1.18	1.01	0.77	1.17	1.01	0.77	1.18	1.00	0.76
22–25	1.18	1.01	0.77	1.15	1.00	0.77	1.16	1.01	0.78	1.16	1.01	0.78	1.16	1.00	0.78
25–28	1.16	1.01	0.79	1.14	1.00	0.79	1.14	1.00	0.80	1.15	1.01	0.79	1.15	1.00	0.79
28–30	1.15	1.01	0.80	1.12	1.00	0.80	1.13	1.00	0.81	1.13	1.00	0.81	1.13	1.00	0.81
30–35	1.14	1.01	0.81	1.12	1.00	0.81	1.12	1.00	0.82	1.12	1.00	0.82	1.12	1.00	0.82
35–40	1.12	1.01	0.83	1.10	1.00	0.83	1.11	1.00	0.84	1.11	1.00	0.84	1.11	1.00	0.83
40–55	1.10	1.00	0.85	1.08	1.00	0.86	1.08	1.00	0.86	1.08	1.00	0.87	1.09	1.00	0.86
55–75	1.07	1.00	0.88	1.07	1.00	0.88	1.06	1.00	0.89	1.06	1.00	0.89	1.07	1.00	0.88
75–100	1.04	1.00	0.92	1.03	1.00	0.93	1.03	1.00	0.94	1.03	1.00	0.92	1.03	1.00	0.93
100–130													1.03	1.00	0.93

Table A.8: Multiplicative scaling factors to obtain the Y(1S) differential cross sections for different polarization scenarios ($\lambda_\theta^{\text{HX}} = +1, k, -1$) from the unpolarized cross section measurements given in Table A.3. The parameter k corresponds to a linear interpolation of the CMS measured value of $\lambda_\theta^{\text{HX}}$ [31] as a function of p_{T} for $p_{\text{T}} < 50\,\text{GeV}$. For $p_{\text{T}} > 50\,\text{GeV}$, where no measurements of $\lambda_\theta^{\text{HX}}$ exist, k is taken as the average of all the measured values of $\lambda_\theta^{\text{HX}}$ for $p_{\text{T}} < 50\,\text{GeV}$.

p_{T} [GeV]	$|y| < 0.6$			$0.6 < |y| < 1.2$			$|y| < 1.2$		
	$\lambda_\theta = +1$	$\lambda_\theta = k$	$\lambda_\theta = -1$	$\lambda_\theta = +1$	$\lambda_\theta = k$	$\lambda_\theta = -1$	$\lambda_\theta = +1$	$\lambda_\theta = k$	$\lambda_\theta = -1$
20–22	1.14	0.98	0.78	1.14	0.98	0.78	1.14	0.98	0.78
22–24	1.13	0.99	0.78	1.13	0.99	0.78	1.13	0.99	0.78
24–26	1.12	0.99	0.79	1.12	0.99	0.79	1.12	0.99	0.79
26–28	1.11	0.99	0.80	1.11	0.99	0.80	1.11	0.99	0.80
28–30	1.11	0.99	0.81	1.11	0.99	0.81	1.11	0.99	0.81
30–32	1.10	1.01	0.81	1.10	1.01	0.81	1.10	1.01	0.81
32–34	1.10	1.01	0.82	1.10	1.01	0.82	1.10	1.01	0.82
34–36	1.09	1.01	0.82	1.09	1.01	0.82	1.09	1.01	0.82
36–38	1.09	1.01	0.83	1.09	1.01	0.83	1.09	1.01	0.83
38–40	1.10	1.01	0.83	1.10	1.01	0.83	1.10	1.01	0.83
40–43	1.08	1.01	0.84	1.08	1.01	0.84	1.08	1.01	0.84
43–46	1.07	1.01	0.85	1.07	1.01	0.85	1.07	1.01	0.85
46–50	1.07	1.01	0.85	1.07	1.01	0.85	1.07	1.01	0.85
50–55	1.06	0.99	0.86	1.06	0.99	0.86	1.06	0.99	0.86
55–60	1.05	0.99	0.88	1.05	0.99	0.88	1.05	0.99	0.88
60–70	1.05	0.99	0.88	1.05	0.99	0.88	1.05	0.99	0.88
70–100	1.03	1.00	0.92	1.03	1.00	0.92	1.03	1.00	0.92
100–130							1.03	1.00	0.92

Table A.9: Multiplicative scaling factors to obtain the $\Upsilon(2S)$ differential cross sections for different polarization scenarios ($\lambda_\theta^{HX} = +1, k, -1$) from the unpolarized cross section measurements given in Table A.4. The parameter k corresponds to a linear interpolation of the CMS measured value of λ_θ^{HX} [31] as a function of p_T for $p_T < 50\,\text{GeV}$. For $p_T > 50\,\text{GeV}$, where no measurements of λ_θ^{HX} exist, k is taken as the average of all the measured values of λ_θ^{HX} for $p_T < 50\,\text{GeV}$.

p_T	$|y| < 0.6$			$0.6 < |y| < 1.2$			$|y| < 1.2$		
[GeV]	$\lambda_\theta = +1$	$\lambda_\theta = k$	$\lambda_\theta = -1$	$\lambda_\theta = +1$	$\lambda_\theta = k$	$\lambda_\theta = -1$	$\lambda_\theta = +1$	$\lambda_\theta = k$	$\lambda_\theta = -1$
20–22	1.14	1.03	0.78	1.14	1.03	0.78	1.14	1.03	0.78
22–24	1.13	1.03	0.79	1.13	1.03	0.79	1.13	1.03	0.79
24–26	1.12	1.03	0.79	1.12	1.03	0.79	1.12	1.03	0.79
26–28	1.11	1.03	0.80	1.11	1.03	0.80	1.11	1.03	0.80
28–30	1.11	1.03	0.81	1.11	1.03	0.81	1.11	1.03	0.81
30–32	1.10	1.03	0.82	1.10	1.03	0.82	1.10	1.03	0.82
32–34	1.10	1.03	0.82	1.10	1.03	0.82	1.10	1.03	0.82
34–36	1.09	1.03	0.82	1.09	1.03	0.82	1.09	1.03	0.82
36–38	1.09	1.03	0.83	1.09	1.03	0.83	1.09	1.03	0.83
38–40	1.09	1.03	0.83	1.09	1.03	0.83	1.09	1.03	0.83
40–43	1.08	1.03	0.84	1.08	1.03	0.84	1.08	1.03	0.84
43–46	1.07	1.02	0.85	1.07	1.02	0.85	1.07	1.02	0.85
46–50	1.07	1.02	0.86	1.07	1.02	0.86	1.07	1.02	0.86
50–55	1.06	0.99	0.87	1.06	0.99	0.87	1.06	0.99	0.87
55–60	1.06	0.99	0.86	1.06	0.99	0.86	1.06	0.99	0.86
60–70	1.05	0.99	0.90	1.05	0.99	0.90	1.05	0.99	0.90
70–100	1.03	0.99	0.92	1.03	0.99	0.92	1.03	0.99	0.92
100–130							1.03	0.99	0.92

Table A.10: Multiplicative scaling factors to obtain the Υ(3S) differential cross sections for different polarization scenarios ($\lambda_\theta^{\text{HX}} = +1, k, -1$) from the unpolarized cross section measurements given in Table A.5. The parameter k corresponds to a linear interpolation of the CMS measured value of $\lambda_\theta^{\text{HX}}$ [31] as a function of p_{T} for $p_{\text{T}} < 50\,\text{GeV}$. For $p_{\text{T}} > 50\,\text{GeV}$, where no measurements of $\lambda_\theta^{\text{HX}}$ exist, k is taken as the average of all the measured values of $\lambda_\theta^{\text{HX}}$ for $p_{\text{T}} < 50\,\text{GeV}$, which are all consistent with a single value.

p_{T} [GeV]	$|y| < 0.6$			$0.6 < |y| < 1.2$			$|y| < 1.2$		
	$\lambda_\theta = +1$	$\lambda_\theta = k$	$\lambda_\theta = -1$	$\lambda_\theta = +1$	$\lambda_\theta = k$	$\lambda_\theta = -1$	$\lambda_\theta = +1$	$\lambda_\theta = k$	$\lambda_\theta = -1$
20–22	1.13	1.03	0.78	1.13	1.03	0.78	1.13	1.03	0.78
22–24	1.13	1.02	0.79	1.13	1.02	0.79	1.13	1.02	0.79
24–26	1.12	1.02	0.79	1.12	1.02	0.79	1.12	1.02	0.79
26–28	1.11	1.02	0.80	1.11	1.02	0.80	1.11	1.02	0.80
28–30	1.11	1.02	0.81	1.11	1.02	0.81	1.11	1.02	0.81
30–32	1.10	1.03	0.82	1.10	1.03	0.82	1.10	1.03	0.82
32–34	1.10	1.03	0.82	1.10	1.03	0.82	1.10	1.03	0.82
34–36	1.09	1.03	0.83	1.09	1.03	0.83	1.09	1.03	0.83
36–38	1.09	1.03	0.83	1.09	1.03	0.83	1.09	1.03	0.83
38–40	1.09	1.03	0.84	1.09	1.03	0.84	1.09	1.03	0.84
40–43	1.08	1.03	0.84	1.08	1.03	0.84	1.08	1.03	0.84
43–46	1.07	1.02	0.85	1.07	1.02	0.85	1.07	1.02	0.85
46–50	1.06	1.02	0.86	1.06	1.02	0.86	1.06	1.02	0.86
50–55	1.06	0.99	0.87	1.06	0.99	0.87	1.06	0.99	0.87
55–60	1.06	0.99	0.87	1.06	0.99	0.87	1.06	0.99	0.87
60–70	1.05	0.99	0.89	1.05	0.99	0.89	1.05	0.99	0.89
70–100	1.03	0.99	0.92	1.03	0.99	0.92	1.03	0.99	0.92
100–130							1.03	0.99	0.92

A   Dimuon invariant mass and lifetime distributions, numerical values of differential cross section, and correction factors for alternative polarization scenarios

24

Table A.11: Ratios of the p_T differential cross sections times dimuon branching fractions of the prompt $\psi(2S)$ to J/ψ, $\Upsilon(2S)$ to $\Upsilon(1S)$, and $\Upsilon(3S)$ to $\Upsilon(1S)$ mesons for $|y| < 1.2$, with their statistical and systematic uncertainties in percent.

p_T [GeV]	$\psi(2S)$ / J/ψ	stat %	syst %
20–21	0.04	3	11
21–22	0.04	3	11
22–23	0.04	3	11
23–24	0.05	3	11
24–25	0.04	4	13
25–26	0.04	4	14
26–27	0.04	5	15
27–28	0.04	5	16
28–29	0.05	5	17
29–30	0.05	6	17
30–32	0.04	5	18
32–34	0.04	6	18
34–36	0.04	6	20
36–38	0.04	7	20
38–42	0.05	6	21
42–46	0.04	9	22
46–50	0.05	10	25
50–60	0.05	10	25
60–75	0.04	42	26
75–95	0.05	10	29
95–120	0.06	21	38
120–150	0.07	71	38

p_T [GeV]	$\Upsilon(2S)$ / $\Upsilon(1S)$	stat %	syst %	$\Upsilon(3S)$ / $\Upsilon(1S)$	stat %	syst %
20–22	0.42	1.7	8.5	0.28	2.0	9.1
22–24	0.43	2.0	8.4	0.31	2.3	7.5
24–26	0.47	2.3	6.9	0.32	2.7	7.1
26–28	0.46	2.8	6.2	0.33	3.1	6.8
28–30	0.45	3.2	6.4	0.33	3.8	8.1
30–32	0.48	3.8	7.8	0.35	4.3	8.9
32–34	0.50	4.3	6.3	0.37	4.9	8.3
34–36	0.51	5.0	7.9	0.38	5.5	11
36–38	0.47	6.1	8.3	0.40	6.4	11
38–40	0.50	6.8	8.3	0.47	6.9	11
40–43	0.48	6.1	5.7	0.36	7.0	7.1
43–46	0.48	7.7	5.4	0.36	8.8	6.6
46–50	0.49	8.3	5.3	0.40	9.0	6.6
50–55	0.52	8.9	5.4	0.43	9.8	7.5
55–60	0.56	11	6.2	0.43	12	9.2
60–70	0.62	11	6.6	0.46	12	11
70–100	0.48	14	6.6	0.46	14	14
100–130	0.89	40	6.6	0.35	52	14

B The CMS Collaboration

Yerevan Physics Institute, Yerevan, Armenia
A.M. Sirunyan, A. Tumasyan

Institut für Hochenergiephysik, Wien, Austria
W. Adam, F. Ambrogi, E. Asilar, T. Bergauer, J. Brandstetter, E. Brondolin, M. Dragicevic, J. Erö, M. Flechl, M. Friedl, R. Frühwirth[1], V.M. Ghete, J. Grossmann, J. Hrubec, M. Jeitler[1], A. König, N. Krammer, I. Krätschmer, D. Liko, T. Madlener, I. Mikulec, E. Pree, D. Rabady, N. Rad, H. Rohringer, J. Schieck[1], R. Schöfbeck, M. Spanring, D. Spitzbart, W. Waltenberger, J. Wittmann, C.-E. Wulz[1], M. Zarucki

Institute for Nuclear Problems, Minsk, Belarus
V. Chekhovsky, V. Mossolov, J. Suarez Gonzalez

Universiteit Antwerpen, Antwerpen, Belgium
E.A. De Wolf, D. Di Croce, X. Janssen, J. Lauwers, M. Van De Klundert, H. Van Haevermaet, P. Van Mechelen, N. Van Remortel

Vrije Universiteit Brussel, Brussel, Belgium
S. Abu Zeid, F. Blekman, J. D'Hondt, I. De Bruyn, J. De Clercq, K. Deroover, G. Flouris, D. Lontkovskyi, S. Lowette, S. Moortgat, L. Moreels, Q. Python, K. Skovpen, S. Tavernier, W. Van Doninck, P. Van Mulders, I. Van Parijs

Université Libre de Bruxelles, Bruxelles, Belgium
H. Brun, B. Clerbaux, G. De Lentdecker, H. Delannoy, G. Fasanella, L. Favart, R. Goldouzian, A. Grebenyuk, G. Karapostoli, T. Lenzi, J. Luetic, T. Maerschalk, A. Marinov, A. Randle-conde, T. Seva, C. Vander Velde, P. Vanlaer, D. Vannerom, R. Yonamine, F. Zenoni, F. Zhang[2]

Ghent University, Ghent, Belgium
A. Cimmino, T. Cornelis, D. Dobur, A. Fagot, M. Gul, I. Khvastunov, D. Poyraz, C. Roskas, S. Salva, M. Tytgat, W. Verbeke, N. Zaganidis

Université Catholique de Louvain, Louvain-la-Neuve, Belgium
H. Bakhshiansohi, O. Bondu, S. Brochet, G. Bruno, C. Caputo, A. Caudron, S. De Visscher, C. Delaere, M. Delcourt, B. Francois, A. Giammanco, A. Jafari, M. Komm, G. Krintiras, V. Lemaitre, A. Magitteri, A. Mertens, M. Musich, K. Piotrzkowski, L. Quertenmont, M. Vidal Marono, S. Wertz

Université de Mons, Mons, Belgium
N. Beliy

Centro Brasileiro de Pesquisas Fisicas, Rio de Janeiro, Brazil
W.L. Aldá Júnior, F.L. Alves, G.A. Alves, L. Brito, M. Correa Martins Junior, C. Hensel, A. Moraes, M.E. Pol, P. Rebello Teles

Universidade do Estado do Rio de Janeiro, Rio de Janeiro, Brazil
E. Belchior Batista Das Chagas, W. Carvalho, J. Chinellato[3], A. Custódio, E.M. Da Costa, G.G. Da Silveira[4], D. De Jesus Damiao, S. Fonseca De Souza, L.M. Huertas Guativa, H. Malbouisson, M. Melo De Almeida, C. Mora Herrera, L. Mundim, H. Nogima, A. Santoro, A. Sznajder, E.J. Tonelli Manganote[3], F. Torres Da Silva De Araujo, A. Vilela Pereira

Universidade Estadual Paulista [a], Universidade Federal do ABC [b], São Paulo, Brazil
S. Ahuja[a], C.A. Bernardes[a], T.R. Fernandez Perez Tomei[a], E.M. Gregores[b], P.G. Mercadante[b], S.F. Novaes[a], Sandra S. Padula[a], D. Romero Abad[b], J.C. Ruiz Vargas[a]

Institute for Nuclear Research and Nuclear Energy, Bulgarian Academy of Sciences, Sofia, Bulgaria
A. Aleksandrov, R. Hadjiiska, P. Iaydjiev, M. Misheva, M. Rodozov, M. Shopova, S. Stoykova, G. Sultanov

University of Sofia, Sofia, Bulgaria
A. Dimitrov, I. Glushkov, L. Litov, B. Pavlov, P. Petkov

Beihang University, Beijing, China
W. Fang[5], X. Gao[5]

Institute of High Energy Physics, Beijing, China
M. Ahmad, J.G. Bian, G.M. Chen, H.S. Chen, M. Chen, Y. Chen, C.H. Jiang, D. Leggat, H. Liao, Z. Liu, F. Romeo, S.M. Shaheen, A. Spiezia, J. Tao, C. Wang, Z. Wang, E. Yazgan, H. Zhang, S. Zhang, J. Zhao

State Key Laboratory of Nuclear Physics and Technology, Peking University, Beijing, China
Y. Ban, G. Chen, Q. Li, S. Liu, Y. Mao, S.J. Qian, D. Wang, Z. Xu

Universidad de Los Andes, Bogota, Colombia
C. Avila, A. Cabrera, L.F. Chaparro Sierra, C. Florez, C.F. González Hernández, J.D. Ruiz Alvarez

University of Split, Faculty of Electrical Engineering, Mechanical Engineering and Naval Architecture, Split, Croatia
B. Courbon, N. Godinovic, D. Lelas, I. Puljak, P.M. Ribeiro Cipriano, T. Sculac

University of Split, Faculty of Science, Split, Croatia
Z. Antunovic, M. Kovac

Institute Rudjer Boskovic, Zagreb, Croatia
V. Brigljevic, D. Ferencek, K. Kadija, B. Mesic, A. Starodumov[6], T. Susa

University of Cyprus, Nicosia, Cyprus
M.W. Ather, A. Attikis, G. Mavromanolakis, J. Mousa, C. Nicolaou, F. Ptochos, P.A. Razis, H. Rykaczewski

Charles University, Prague, Czech Republic
M. Finger[7], M. Finger Jr.[7]

Universidad San Francisco de Quito, Quito, Ecuador
E. Carrera Jarrin

Academy of Scientific Research and Technology of the Arab Republic of Egypt, Egyptian Network of High Energy Physics, Cairo, Egypt
Y. Assran[8,9], S. Elgammal[9], A. Mahrous[10]

National Institute of Chemical Physics and Biophysics, Tallinn, Estonia
R.K. Dewanjee, M. Kadastik, L. Perrini, M. Raidal, A. Tiko, C. Veelken

Department of Physics, University of Helsinki, Helsinki, Finland
P. Eerola, J. Pekkanen, M. Voutilainen

Helsinki Institute of Physics, Helsinki, Finland
J. Härkönen, T. Järvinen, V. Karimäki, R. Kinnunen, T. Lampén, K. Lassila-Perini, S. Lehti, T. Lindén, P. Luukka, E. Tuominen, J. Tuominiemi, E. Tuovinen

Lappeenranta University of Technology, Lappeenranta, Finland
J. Talvitie, T. Tuuva

IRFU, CEA, Université Paris-Saclay, Gif-sur-Yvette, France
M. Besancon, F. Couderc, M. Dejardin, D. Denegri, J.L. Faure, F. Ferri, S. Ganjour, S. Ghosh, A. Givernaud, P. Gras, G. Hamel de Monchenault, P. Jarry, I. Kucher, E. Locci, M. Machet, J. Malcles, G. Negro, J. Rander, A. Rosowsky, M.Ö. Sahin, M. Titov

Laboratoire Leprince-Ringuet, Ecole polytechnique, CNRS/IN2P3, Université Paris-Saclay, Palaiseau, France
A. Abdulsalam, I. Antropov, S. Baffioni, F. Beaudette, P. Busson, L. Cadamuro, C. Charlot, R. Granier de Cassagnac, M. Jo, S. Lisniak, A. Lobanov, J. Martin Blanco, M. Nguyen, C. Ochando, G. Ortona, P. Paganini, P. Pigard, S. Regnard, R. Salerno, J.B. Sauvan, Y. Sirois, A.G. Stahl Leiton, T. Strebler, Y. Yilmaz, A. Zabi, A. Zghiche

Université de Strasbourg, CNRS, IPHC UMR 7178, F-67000 Strasbourg, France
J.-L. Agram[11], J. Andrea, D. Bloch, J.-M. Brom, M. Buttignol, E.C. Chabert, N. Chanon, C. Collard, E. Conte[11], X. Coubez, J.-C. Fontaine[11], D. Gelé, U. Goerlach, M. Jansová, A.-C. Le Bihan, N. Tonon, P. Van Hove

Centre de Calcul de l'Institut National de Physique Nucleaire et de Physique des Particules, CNRS/IN2P3, Villeurbanne, France
S. Gadrat

Université de Lyon, Université Claude Bernard Lyon 1, CNRS-IN2P3, Institut de Physique Nucléaire de Lyon, Villeurbanne, France
S. Beauceron, C. Bernet, G. Boudoul, R. Chierici, D. Contardo, P. Depasse, H. El Mamouni, J. Fay, L. Finco, S. Gascon, M. Gouzevitch, G. Grenier, B. Ille, F. Lagarde, I.B. Laktineh, M. Lethuillier, L. Mirabito, A.L. Pequegnot, S. Perries, A. Popov[12], V. Sordini, M. Vander Donckt, S. Viret

Georgian Technical University, Tbilisi, Georgia
A. Khvedelidze[7]

Tbilisi State University, Tbilisi, Georgia
I. Bagaturia[13]

RWTH Aachen University, I. Physikalisches Institut, Aachen, Germany
C. Autermann, S. Beranek, L. Feld, M.K. Kiesel, K. Klein, M. Lipinski, M. Preuten, C. Schomakers, J. Schulz, T. Verlage, V. Zhukov[12]

RWTH Aachen University, III. Physikalisches Institut A, Aachen, Germany
A. Albert, E. Dietz-Laursonn, D. Duchardt, M. Endres, M. Erdmann, S. Erdweg, T. Esch, R. Fischer, A. Güth, M. Hamer, T. Hebbeker, C. Heidemann, K. Hoepfner, S. Knutzen, M. Merschmeyer, A. Meyer, P. Millet, S. Mukherjee, M. Olschewski, K. Padeken, T. Pook, M. Radziej, H. Reithler, M. Rieger, F. Scheuch, D. Teyssier, S. Thüer

RWTH Aachen University, III. Physikalisches Institut B, Aachen, Germany
G. Flügge, B. Kargoll, T. Kress, A. Künsken, J. Lingemann, T. Müller, A. Nehrkorn, A. Nowack, C. Pistone, O. Pooth, A. Stahl[14]

Deutsches Elektronen-Synchrotron, Hamburg, Germany
M. Aldaya Martin, T. Arndt, C. Asawatangtrakuldee, K. Beernaert, O. Behnke, U. Behrens, A. Bermúdez Martínez, A.A. Bin Anuar, K. Borras[15], V. Botta, A. Campbell, P. Connor, C. Contreras-Campana, F. Costanza, C. Diez Pardos, G. Eckerlin, D. Eckstein, T. Eichhorn,

E. Eren, E. Gallo[16], J. Garay Garcia, A. Geiser, A. Gizhko, J.M. Grados Luyando, A. Grohsjean, P. Gunnellini, M. Guthoff, A. Harb, J. Hauk, M. Hempel[17], H. Jung, A. Kalogeropoulos, M. Kasemann, J. Keaveney, C. Kleinwort, I. Korol, D. Krücker, W. Lange, A. Lelek, T. Lenz, J. Leonard, K. Lipka, W. Lohmann[17], R. Mankel, I.-A. Melzer-Pellmann, A.B. Meyer, G. Mittag, J. Mnich, A. Mussgiller, E. Ntomari, D. Pitzl, A. Raspereza, B. Roland, M. Savitskyi, P. Saxena, R. Shevchenko, S. Spannagel, N. Stefaniuk, G.P. Van Onsem, R. Walsh, Y. Wen, K. Wichmann, C. Wissing, O. Zenaiev

University of Hamburg, Hamburg, Germany
S. Bein, V. Blobel, M. Centis Vignali, T. Dreyer, E. Garutti, D. Gonzalez, J. Haller, A. Hinzmann, M. Hoffmann, A. Karavdina, R. Klanner, R. Kogler, N. Kovalchuk, S. Kurz, T. Lapsien, I. Marchesini, D. Marconi, M. Meyer, M. Niedziela, D. Nowatschin, F. Pantaleo[14], T. Peiffer, A. Perieanu, C. Scharf, P. Schleper, A. Schmidt, S. Schumann, J. Schwandt, J. Sonneveld, H. Stadie, G. Steinbrück, F.M. Stober, M. Stöver, H. Tholen, D. Troendle, E. Usai, L. Vanelderen, A. Vanhoefer, B. Vormwald

Institut für Experimentelle Kernphysik, Karlsruhe, Germany
M. Akbiyik, C. Barth, S. Baur, E. Butz, R. Caspart, T. Chwalek, F. Colombo, W. De Boer, A. Dierlamm, B. Freund, R. Friese, M. Giffels, A. Gilbert, D. Haitz, F. Hartmann[14], S.M. Heindl, U. Husemann, F. Kassel[14], S. Kudella, H. Mildner, M.U. Mozer, Th. Müller, M. Plagge, G. Quast, K. Rabbertz, M. Schröder, I. Shvetsov, G. Sieber, H.J. Simonis, R. Ulrich, S. Wayand, M. Weber, T. Weiler, S. Williamson, C. Wöhrmann, R. Wolf

Institute of Nuclear and Particle Physics (INPP),   NCSR Demokritos, Aghia Paraskevi, Greece
G. Anagnostou, G. Daskalakis, T. Geralis, V.A. Giakoumopoulou, A. Kyriakis, D. Loukas, I. Topsis-Giotis

National and Kapodistrian University of Athens, Athens, Greece
G. Karathanasis, S. Kesisoglou, A. Panagiotou, N. Saoulidou

National Technical University of Athens, Athens, Greece
K. Kousouris

University of Ioánnina, Ioánnina, Greece
I. Evangelou, C. Foudas, P. Kokkas, S. Mallios, N. Manthos, I. Papadopoulos, E. Paradas, J. Strologas, F.A. Triantis

MTA-ELTE Lendület CMS Particle and Nuclear Physics Group, Eötvös Loránd University, Budapest, Hungary
M. Csanad, N. Filipovic, G. Pasztor, G.I. Veres[18]

Wigner Research Centre for Physics, Budapest, Hungary
G. Bencze, C. Hajdu, D. Horvath[19], Á. Hunyadi, F. Sikler, V. Veszpremi, A.J. Zsigmond

Institute of Nuclear Research ATOMKI, Debrecen, Hungary
N. Beni, S. Czellar, J. Karancsi[20], A. Makovec, J. Molnar, Z. Szillasi

Institute of Physics, University of Debrecen, Debrecen, Hungary
M. Bartók[18], P. Raics, Z.L. Trocsanyi, B. Ujvari

Indian Institute of Science (IISc), Bangalore, India
S. Choudhury, J.R. Komaragiri

National Institute of Science Education and Research, Bhubaneswar, India
S. Bahinipati[21], S. Bhowmik, P. Mal, K. Mandal, A. Nayak[22], D.K. Sahoo[21], N. Sahoo, S.K. Swain

Panjab University, Chandigarh, India
S. Bansal, S.B. Beri, V. Bhatnagar, R. Chawla, N. Dhingra, A.K. Kalsi, A. Kaur, M. Kaur, R. Kumar, P. Kumari, A. Mehta, J.B. Singh, G. Walia

University of Delhi, Delhi, India
Ashok Kumar, Aashaq Shah, A. Bhardwaj, S. Chauhan, B.C. Choudhary, R.B. Garg, S. Keshri, A. Kumar, S. Malhotra, M. Naimuddin, K. Ranjan, R. Sharma

Saha Institute of Nuclear Physics, HBNI, Kolkata, India
R. Bhardwaj, R. Bhattacharya, S. Bhattacharya, U. Bhawandeep, S. Dey, S. Dutt, S. Dutta, S. Ghosh, N. Majumdar, A. Modak, K. Mondal, S. Mukhopadhyay, S. Nandan, A. Purohit, A. Roy, D. Roy, S. Roy Chowdhury, S. Sarkar, M. Sharan, S. Thakur

Indian Institute of Technology Madras, Madras, India
P.K. Behera

Bhabha Atomic Research Centre, Mumbai, India
R. Chudasama, D. Dutta, V. Jha, V. Kumar, A.K. Mohanty[14], P.K. Netrakanti, L.M. Pant, P. Shukla, A. Topkar

Tata Institute of Fundamental Research-A, Mumbai, India
T. Aziz, S. Dugad, B. Mahakud, S. Mitra, G.B. Mohanty, N. Sur, B. Sutar

Tata Institute of Fundamental Research-B, Mumbai, India
S. Banerjee, S. Bhattacharya, S. Chatterjee, P. Das, M. Guchait, Sa. Jain, S. Kumar, M. Maity[23], G. Majumder, K. Mazumdar, T. Sarkar[23], N. Wickramage[24]

Indian Institute of Science Education and Research (IISER), Pune, India
S. Chauhan, S. Dube, V. Hegde, A. Kapoor, K. Kothekar, S. Pandey, A. Rane, S. Sharma

Institute for Research in Fundamental Sciences (IPM), Tehran, Iran
S. Chenarani[25], E. Eskandari Tadavani, S.M. Etesami[25], M. Khakzad, M. Mohammadi Najafabadi, M. Naseri, S. Paktinat Mehdiabadi[26], F. Rezaei Hosseinabadi, B. Safarzadeh[27], M. Zeinali

University College Dublin, Dublin, Ireland
M. Felcini, M. Grunewald

INFN Sezione di Bari [a], Università di Bari [b], Politecnico di Bari [c], Bari, Italy
M. Abbrescia[a,b], C. Calabria[a,b], A. Colaleo[a], D. Creanza[a,c], L. Cristella[a,b], N. De Filippis[a,c], M. De Palma[a,b], F. Errico[a,b], L. Fiore[a], G. Iaselli[a,c], S. Lezki[a,b], G. Maggi[a,c], M. Maggi[a], G. Miniello[a,b], S. My[a,b], S. Nuzzo[a,b], A. Pompili[a,b], G. Pugliese[a,c], R. Radogna[a], A. Ranieri[a], G. Selvaggi[a,b], A. Sharma[a], L. Silvestris[a,14], R. Venditti[a], P. Verwilligen[a]

INFN Sezione di Bologna [a], Università di Bologna [b], Bologna, Italy
G. Abbiendi[a], C. Battilana[a,b], D. Bonacorsi[a,b], S. Braibant-Giacomelli[a,b], R. Campanini[a,b], P. Capiluppi[a,b], A. Castro[a,b], F.R. Cavallo[a], S.S. Chhibra[a], G. Codispoti[a,b], M. Cuffiani[a,b], G.M. Dallavalle[a], F. Fabbri[a], A. Fanfani[a,b], D. Fasanella[a,b], P. Giacomelli[a], C. Grandi[a], L. Guiducci[a,b], S. Marcellini[a], G. Masetti[a], A. Montanari[a], F.L. Navarria[a,b], A. Perrotta[a], A.M. Rossi[a,b], T. Rovelli[a,b], G.P. Siroli[a,b], N. Tosi[a]

INFN Sezione di Catania [a], Università di Catania [b], Catania, Italy
S. Albergo[a,b], S. Costa[a,b], A. Di Mattia[a], F. Giordano[a,b], R. Potenza[a,b], A. Tricomi[a,b], C. Tuve[a,b]

INFN Sezione di Firenze ^{a}, Università di Firenze ^{b}, Firenze, Italy
G. Barbagli^a, K. Chatterjee^{a,b}, V. Ciulli^{a,b}, C. Civinini^a, R. D'Alessandro^{a,b}, E. Focardi^{a,b}, P. Lenzi^{a,b}, M. Meschini^a, S. Paoletti^a, L. Russo^{a,28}, G. Sguazzoni^a, D. Strom^a, L. Viliani^{a,b,14}

INFN Laboratori Nazionali di Frascati, Frascati, Italy
L. Benussi, S. Bianco, F. Fabbri, D. Piccolo, F. Primavera^{14}

INFN Sezione di Genova ^{a}, Università di Genova ^{b}, Genova, Italy
V. Calvelli^{a,b}, F. Ferro^a, E. Robutti^a, S. Tosi^{a,b}

INFN Sezione di Milano-Bicocca ^{a}, Università di Milano-Bicocca ^{b}, Milano, Italy
A. Benaglia^a, L. Brianza^{a,b}, F. Brivio^{a,b}, V. Ciriolo^{a,b}, M.E. Dinardo^{a,b}, S. Fiorendi^{a,b}, S. Gennai^a, A. Ghezzi^{a,b}, P. Govoni^{a,b}, M. Malberti^{a,b}, S. Malvezzi^a, R.A. Manzoni^{a,b}, D. Menasce^a, L. Moroni^a, M. Paganoni^{a,b}, K. Pauwels^{a,b}, D. Pedrini^a, S. Pigazzini^{a,b,29}, S. Ragazzi^{a,b}, T. Tabarelli de Fatis^{a,b}

INFN Sezione di Napoli ^{a}, Università di Napoli 'Federico II' ^{b}, Napoli, Italy, Università della Basilicata ^{c}, Potenza, Italy, Università G. Marconi ^{d}, Roma, Italy
S. Buontempo^a, N. Cavallo^{a,c}, S. Di Guida^{a,d,14}, F. Fabozzi^{a,c}, F. Fienga^{a,b}, A.O.M. Iorio^{a,b}, W.A. Khan^a, L. Lista^a, S. Meola^{a,d,14}, P. Paolucci^{a,14}, C. Sciacca^{a,b}, F. Thyssen^a

INFN Sezione di Padova ^{a}, Università di Padova ^{b}, Padova, Italy, Università di Trento ^{c}, Trento, Italy
P. Azzi^{a,14}, N. Bacchetta^a, L. Benato^{a,b}, D. Bisello^{a,b}, A. Boletti^{a,b}, R. Carlin^{a,b}, A. Carvalho Antunes De Oliveira^{a,b}, P. Checchia^a, M. Dall'Osso^{a,b}, P. De Castro Manzano^a, T. Dorigo^a, U. Dosselli^a, F. Gasparini^{a,b}, U. Gasparini^{a,b}, A. Gozzelino^a, S. Lacaprara^a, P. Lujan, M. Margoni^{a,b}, A.T. Meneguzzo^{a,b}, N. Pozzobon^{a,b}, P. Ronchese^{a,b}, R. Rossin^{a,b}, F. Simonetto^{a,b}, E. Torassa^a, S. Ventura^a, P. Zotto^{a,b}

INFN Sezione di Pavia ^{a}, Università di Pavia ^{b}, Pavia, Italy
A. Braghieri^a, A. Magnani^{a,b}, P. Montagna^{a,b}, S.P. Ratti^{a,b}, V. Re^a, M. Ressegotti, C. Riccardi^{a,b}, P. Salvini^a, I. Vai^{a,b}, P. Vitulo^{a,b}

INFN Sezione di Perugia ^{a}, Università di Perugia ^{b}, Perugia, Italy
L. Alunni Solestizi^{a,b}, M. Biasini^{a,b}, G.M. Bilei^a, C. Cecchi^{a,b}, D. Ciangottini^{a,b}, L. Fanò^{a,b}, P. Lariccia^{a,b}, R. Leonardi^{a,b}, E. Manoni^a, G. Mantovani^{a,b}, V. Mariani^{a,b}, M. Menichelli^a, A. Rossi^{a,b}, A. Santocchia^{a,b}, D. Spiga^a

INFN Sezione di Pisa ^{a}, Università di Pisa ^{b}, Scuola Normale Superiore di Pisa ^{c}, Pisa, Italy
K. Androsov^a, P. Azzurri^{a,14}, G. Bagliesi^a, T. Boccali^a, L. Borrello, R. Castaldi^a, M.A. Ciocci^{a,b}, R. Dell'Orso^a, G. Fedi^a, L. Giannini^{a,c}, A. Giassi^a, M.T. Grippo^{a,28}, F. Ligabue^{a,c}, T. Lomtadze^a, E. Manca^{a,c}, G. Mandorli^{a,c}, L. Martini^{a,b}, A. Messineo^{a,b}, F. Palla^a, A. Rizzi^{a,b}, A. Savoy-Navarro^{a,30}, P. Spagnolo^a, R. Tenchini^a, G. Tonelli^{a,b}, A. Venturi^a, P.G. Verdini^a

INFN Sezione di Roma ^{a}, Sapienza Università di Roma ^{b}, Rome, Italy
L. Barone^{a,b}, F. Cavallari^a, M. Cipriani^{a,b}, N. Daci^a, D. Del Re^{a,b,14}, E. Di Marco^{a,b}, M. Diemoz^a, S. Gelli^{a,b}, E. Longo^{a,b}, F. Margaroli^{a,b}, B. Marzocchi^{a,b}, P. Meridiani^a, G. Organtini^{a,b}, R. Paramatti^{a,b}, F. Preiato^{a,b}, S. Rahatlou^{a,b}, C. Rovelli^a, F. Santanastasio^{a,b}

INFN Sezione di Torino ^{a}, Università di Torino ^{b}, Torino, Italy, Università del Piemonte Orientale ^{c}, Novara, Italy
N. Amapane^{a,b}, R. Arcidiacono^{a,c}, S. Argiro^{a,b}, M. Arneodo^{a,c}, N. Bartosik^a, R. Bellan^{a,b}, C. Biino^a, N. Cartiglia^a, M. Costa^{a,b}, R. Covarelli^{a,b}, P. De Remigis^a, A. Degano^{a,b}, N. Demaria^a, B. Kiani^{a,b}, C. Mariotti^a, S. Maselli^a, E. Migliore^{a,b}, V. Monaco^{a,b}, E. Monteil^{a,b}, M. Monteno^a,

M.M. Obertino[a,b], L. Pacher[a,b], N. Pastrone[a], M. Pelliccioni[a], G.L. Pinna Angioni[a,b], F. Ravera[a,b], A. Romero[a,b], M. Ruspa[a,c], R. Sacchi[a,b], K. Shchelina[a,b], V. Sola[a], A. Solano[a,b], A. Staiano[a], P. Traczyk[a,b]

INFN Sezione di Trieste [a]**, Università di Trieste** [b]**, Trieste, Italy**
S. Belforte[a], M. Casarsa[a], F. Cossutti[a], G. Della Ricca[a,b], A. Zanetti[a]

Kyungpook National University, Daegu, Korea
D.H. Kim, G.N. Kim, M.S. Kim, J. Lee, S. Lee, S.W. Lee, C.S. Moon, Y.D. Oh, S. Sekmen, D.C. Son, Y.C. Yang

Chonbuk National University, Jeonju, Korea
A. Lee

Chonnam National University, Institute for Universe and Elementary Particles, Kwangju, Korea
H. Kim, D.H. Moon, G. Oh

Hanyang University, Seoul, Korea
J.A. Brochero Cifuentes, J. Goh, T.J. Kim

Korea University, Seoul, Korea
S. Cho, S. Choi, Y. Go, D. Gyun, S. Ha, B. Hong, Y. Jo, Y. Kim, K. Lee, K.S. Lee, S. Lee, J. Lim, S.K. Park, Y. Roh

Seoul National University, Seoul, Korea
J. Almond, J. Kim, J.S. Kim, H. Lee, K. Lee, K. Nam, S.B. Oh, B.C. Radburn-Smith, S.h. Seo, U.K. Yang, H.D. Yoo, G.B. Yu

University of Seoul, Seoul, Korea
M. Choi, H. Kim, J.H. Kim, J.S.H. Lee, I.C. Park

Sungkyunkwan University, Suwon, Korea
Y. Choi, C. Hwang, J. Lee, I. Yu

Vilnius University, Vilnius, Lithuania
V. Dudenas, A. Juodagalvis, J. Vaitkus

National Centre for Particle Physics, Universiti Malaya, Kuala Lumpur, Malaysia
I. Ahmed, Z.A. Ibrahim, M.A.B. Md Ali[31], F. Mohamad Idris[32], W.A.T. Wan Abdullah, M.N. Yusli, Z. Zolkapli

Centro de Investigacion y de Estudios Avanzados del IPN, Mexico City, Mexico
Reyes-Almanza, R, Ramirez-Sanchez, G., Duran-Osuna, M. C., H. Castilla-Valdez, E. De La Cruz-Burelo, I. Heredia-De La Cruz[33], Rabadan-Trejo, R. I., R. Lopez-Fernandez, J. Mejia Guisao, A. Sanchez-Hernandez, C.H. Zepeda Fernandez

Universidad Iberoamericana, Mexico City, Mexico
S. Carrillo Moreno, C. Oropeza Barrera, F. Vazquez Valencia

Benemerita Universidad Autonoma de Puebla, Puebla, Mexico
I. Pedraza, H.A. Salazar Ibarguen, C. Uribe Estrada

Universidad Autónoma de San Luis Potosí, San Luis Potosí, Mexico
A. Morelos Pineda

University of Auckland, Auckland, New Zealand
D. Krofcheck

University of Canterbury, Christchurch, New Zealand
P.H. Butler

National Centre for Physics, Quaid-I-Azam University, Islamabad, Pakistan
A. Ahmad, M. Ahmad, Q. Hassan, H.R. Hoorani, A. Saddique, M.A. Shah, M. Shoaib, M. Waqas

National Centre for Nuclear Research, Swierk, Poland
H. Bialkowska, M. Bluj, B. Boimska, T. Frueboes, M. Górski, M. Kazana, K. Nawrocki,
M. Szleper, P. Zalewski

Institute of Experimental Physics, Faculty of Physics, University of Warsaw, Warsaw, Poland
K. Bunkowski, A. Byszuk[34], K. Doroba, A. Kalinowski, M. Konecki, J. Krolikowski, M. Misiura,
M. Olszewski, A. Pyskir, M. Walczak

Laboratório de Instrumentação e Física Experimental de Partículas, Lisboa, Portugal
P. Bargassa, C. Beirão Da Cruz E Silva, A. Di Francesco, P. Faccioli, B. Galinhas, M. Gallinaro,
J. Hollar, N. Leonardo, L. Lloret Iglesias, M.V. Nemallapudi, J. Seixas, G. Strong, O. Toldaiev,
D. Vadruccio, J. Varela

Joint Institute for Nuclear Research, Dubna, Russia
A. Baginyan, A. Golunov, I. Golutvin, A. Kamenev, V. Karjavin, I. Kashunin, V. Korenkov,
G. Kozlov, A. Lanev, A. Malakhov, V. Matveev[35,36], V. Palichik, V. Perelygin, S. Shmatov,
V. Smirnov, V. Trofimov, B.S. Yuldashev[37], A. Zarubin

Petersburg Nuclear Physics Institute, Gatchina (St. Petersburg), Russia
Y. Ivanov, V. Kim[38], E. Kuznetsova[39], P. Levchenko, V. Murzin, V. Oreshkin, I. Smirnov,
V. Sulimov, L. Uvarov, S. Vavilov, A. Vorobyev

Institute for Nuclear Research, Moscow, Russia
Yu. Andreev, A. Dermenev, S. Gninenko, N. Golubev, A. Karneyeu, M. Kirsanov, N. Krasnikov,
A. Pashenkov, D. Tlisov, A. Toropin

Institute for Theoretical and Experimental Physics, Moscow, Russia
V. Epshteyn, V. Gavrilov, N. Lychkovskaya, V. Popov, I. Pozdnyakov, G. Safronov,
A. Spiridonov, A. Stepennov, M. Toms, E. Vlasov, A. Zhokin

Moscow Institute of Physics and Technology, Moscow, Russia
T. Aushev, A. Bylinkin[36]

National Research Nuclear University 'Moscow Engineering Physics Institute' (MEPhI), Moscow, Russia
R. Chistov[40], M. Danilov[40], P. Parygin, D. Philippov, S. Polikarpov, E. Tarkovskii

P.N. Lebedev Physical Institute, Moscow, Russia
V. Andreev, M. Azarkin[36], I. Dremin[36], M. Kirakosyan[36], A. Terkulov

Skobeltsyn Institute of Nuclear Physics, Lomonosov Moscow State University, Moscow, Russia
A. Baskakov, A. Belyaev, E. Boos, M. Dubinin[41], L. Dudko, A. Ershov, A. Gribushin,
V. Klyukhin, O. Kodolova, I. Lokhtin, I. Miagkov, S. Obraztsov, S. Petrushanko, V. Savrin,
A. Snigirev

Novosibirsk State University (NSU), Novosibirsk, Russia
V. Blinov[42], Y.Skovpen[42], D. Shtol[42]

State Research Center of Russian Federation, Institute for High Energy Physics, Protvino, Russia
I. Azhgirey, I. Bayshev, S. Bitioukov, D. Elumakhov, V. Kachanov, A. Kalinin, D. Konstantinov, V. Krychkine, V. Petrov, R. Ryutin, A. Sobol, S. Troshin, N. Tyurin, A. Uzunian, A. Volkov

University of Belgrade, Faculty of Physics and Vinca Institute of Nuclear Sciences, Belgrade, Serbia
P. Adzic[43], P. Cirkovic, D. Devetak, M. Dordevic, J. Milosevic, V. Rekovic

Centro de Investigaciones Energéticas Medioambientales y Tecnológicas (CIEMAT), Madrid, Spain
J. Alcaraz Maestre, M. Barrio Luna, M. Cerrada, N. Colino, B. De La Cruz, A. Delgado Peris, A. Escalante Del Valle, C. Fernandez Bedoya, J.P. Fernández Ramos, J. Flix, M.C. Fouz, P. Garcia-Abia, O. Gonzalez Lopez, S. Goy Lopez, J.M. Hernandez, M.I. Josa, A. Pérez-Calero Yzquierdo, J. Puerta Pelayo, A. Quintario Olmeda, I. Redondo, L. Romero, M.S. Soares, A. Álvarez Fernández

Universidad Autónoma de Madrid, Madrid, Spain
C. Albajar, J.F. de Trocóniz, M. Missiroli, D. Moran

Universidad de Oviedo, Oviedo, Spain
J. Cuevas, C. Erice, J. Fernandez Menendez, I. Gonzalez Caballero, J.R. González Fernández, E. Palencia Cortezon, S. Sanchez Cruz, P. Vischia, J.M. Vizan Garcia

Instituto de Física de Cantabria (IFCA), CSIC-Universidad de Cantabria, Santander, Spain
I.J. Cabrillo, A. Calderon, B. Chazin Quero, E. Curras, J. Duarte Campderros, M. Fernandez, J. Garcia-Ferrero, G. Gomez, A. Lopez Virto, J. Marco, C. Martinez Rivero, P. Martinez Ruiz del Arbol, F. Matorras, J. Piedra Gomez, T. Rodrigo, A. Ruiz-Jimeno, L. Scodellaro, N. Trevisani, I. Vila, R. Vilar Cortabitarte

CERN, European Organization for Nuclear Research, Geneva, Switzerland
D. Abbaneo, E. Auffray, P. Baillon, A.H. Ball, D. Barney, M. Bianco, P. Bloch, A. Bocci, C. Botta, T. Camporesi, R. Castello, M. Cepeda, G. Cerminara, E. Chapon, Y. Chen, D. d'Enterria, A. Dabrowski, V. Daponte, A. David, M. De Gruttola, A. De Roeck, M. Dobson, B. Dorney, T. du Pree, M. Dünser, N. Dupont, A. Elliott-Peisert, P. Everaerts, F. Fallavollita, G. Franzoni, J. Fulcher, W. Funk, D. Gigi, K. Gill, F. Glege, D. Gulhan, P. Harris, J. Hegeman, V. Innocente, P. Janot, O. Karacheban[17], J. Kieseler, H. Kirschenmann, V. Knünz, A. Kornmayer[14], M.J. Kortelainen, M. Krammer[1], C. Lange, P. Lecoq, C. Lourenço, M.T. Lucchini, L. Malgeri, M. Mannelli, A. Martelli, F. Meijers, J.A. Merlin, S. Mersi, E. Meschi, P. Milenovic[44], F. Moortgat, M. Mulders, H. Neugebauer, S. Orfanelli, L. Orsini, L. Pape, E. Perez, M. Peruzzi, A. Petrilli, G. Petrucciani, A. Pfeiffer, M. Pierini, A. Racz, T. Reis, G. Rolandi[45], M. Rovere, H. Sakulin, C. Schäfer, C. Schwick, M. Seidel, M. Selvaggi, A. Sharma, P. Silva, P. Sphicas[46], A. Stakia, J. Steggemann, M. Stoye, M. Tosi, D. Treille, A. Triossi, A. Tsirou, V. Veckalns[47], M. Verweij, W.D. Zeuner

Paul Scherrer Institut, Villigen, Switzerland
W. Bertl[†], L. Caminada[48], K. Deiters, W. Erdmann, R. Horisberger, Q. Ingram, H.C. Kaestli, D. Kotlinski, U. Langenegger, T. Rohe, S.A. Wiederkehr

ETH Zurich - Institute for Particle Physics and Astrophysics (IPA), Zurich, Switzerland
F. Bachmair, L. Bäni, P. Berger, L. Bianchini, B. Casal, G. Dissertori, M. Dittmar, M. Donegà,

C. Grab, C. Heidegger, D. Hits, J. Hoss, G. Kasieczka, T. Klijnsma, W. Lustermann, B. Mangano, M. Marionneau, M.T. Meinhard, D. Meister, F. Micheli, P. Musella, F. Nessi-Tedaldi, F. Pandolfi, J. Pata, F. Pauss, G. Perrin, L. Perrozzi, M. Quittnat, M. Reichmann, M. Schönenberger, L. Shchutska, V.R. Tavolaro, K. Theofilatos, M.L. Vesterbacka Olsson, R. Wallny, D.H. Zhu

Universität Zürich, Zurich, Switzerland
T.K. Aarrestad, C. Amsler[49], M.F. Canelli, A. De Cosa, R. Del Burgo, S. Donato, C. Galloni, T. Hreus, B. Kilminster, J. Ngadiuba, D. Pinna, G. Rauco, P. Robmann, D. Salerno, C. Seitz, Y. Takahashi, A. Zucchetta

National Central University, Chung-Li, Taiwan
V. Candelise, T.H. Doan, Sh. Jain, R. Khurana, C.M. Kuo, W. Lin, A. Pozdnyakov, S.S. Yu

National Taiwan University (NTU), Taipei, Taiwan
Arun Kumar, P. Chang, Y. Chao, K.F. Chen, P.H. Chen, F. Fiori, W.-S. Hou, Y. Hsiung, Y.F. Liu, R.-S. Lu, E. Paganis, A. Psallidas, A. Steen, J.f. Tsai

Chulalongkorn University, Faculty of Science, Department of Physics, Bangkok, Thailand
B. Asavapibhop, K. Kovitanggoon, G. Singh, N. Srimanobhas

Çukurova University, Physics Department, Science and Art Faculty, Adana, Turkey
M.N. Bakirci[50], F. Boran, S. Damarseckin, Z.S. Demiroglu, C. Dozen, I. Dumanoglu, E. Eskut, S. Girgis, G. Gokbulut, Y. Guler, I. Hos[51], E.E. Kangal[52], O. Kara, U. Kiminsu, M. Oglakci, G. Onengut[53], K. Ozdemir[54], S. Ozturk[50], H. Topakli[50], S. Turkcapar, I.S. Zorbakir, C. Zorbilmez

Middle East Technical University, Physics Department, Ankara, Turkey
B. Bilin, G. Karapinar[55], K. Ocalan[56], M. Yalvac, M. Zeyrek

Bogazici University, Istanbul, Turkey
E. Gülmez, M. Kaya[57], O. Kaya[58], S. Tekten, E.A. Yetkin[59]

Istanbul Technical University, Istanbul, Turkey
M.N. Agaras, S. Atay, A. Cakir, K. Cankocak

Institute for Scintillation Materials of National Academy of Science of Ukraine, Kharkov, Ukraine
B. Grynyov

National Scientific Center, Kharkov Institute of Physics and Technology, Kharkov, Ukraine
L. Levchuk, P. Sorokin

University of Bristol, Bristol, United Kingdom
R. Aggleton, F. Ball, L. Beck, J.J. Brooke, D. Burns, E. Clement, D. Cussans, O. Davignon, H. Flacher, J. Goldstein, M. Grimes, G.P. Heath, H.F. Heath, J. Jacob, L. Kreczko, C. Lucas, D.M. Newbold[60], S. Paramesvaran, A. Poll, T. Sakuma, S. Seif El Nasr-storey, D. Smith, V.J. Smith

Rutherford Appleton Laboratory, Didcot, United Kingdom
K.W. Bell, A. Belyaev[61], C. Brew, R.M. Brown, L. Calligaris, D. Cieri, D.J.A. Cockerill, J.A. Coughlan, K. Harder, S. Harper, E. Olaiya, D. Petyt, C.H. Shepherd-Themistocleous, A. Thea, I.R. Tomalin, T. Williams

Imperial College, London, United Kingdom
G. Auzinger, R. Bainbridge, S. Breeze, O. Buchmuller, A. Bundock, S. Casasso, M. Citron, D. Colling, L. Corpe, P. Dauncey, G. Davies, A. De Wit, M. Della Negra, R. Di Maria, A. Elwood, Y. Haddad, G. Hall, G. Iles, T. James, R. Lane, C. Laner, L. Lyons, A.-M. Magnan,

S. Malik, L. Mastrolorenzo, T. Matsushita, J. Nash, A. Nikitenko[6], V. Palladino, M. Pesaresi, D.M. Raymond, A. Richards, A. Rose, E. Scott, C. Seez, A. Shtipliyski, S. Summers, A. Tapper, K. Uchida, M. Vazquez Acosta[62], T. Virdee[14], N. Wardle, D. Winterbottom, J. Wright, S.C. Zenz

Brunel University, Uxbridge, United Kingdom
J.E. Cole, P.R. Hobson, A. Khan, P. Kyberd, I.D. Reid, P. Symonds, L. Teodorescu, M. Turner

Baylor University, Waco, USA
A. Borzou, K. Call, J. Dittmann, K. Hatakeyama, H. Liu, N. Pastika, C. Smith

Catholic University of America, Washington DC, USA
R. Bartek, A. Dominguez

The University of Alabama, Tuscaloosa, USA
A. Buccilli, S.I. Cooper, C. Henderson, P. Rumerio, C. West

Boston University, Boston, USA
D. Arcaro, A. Avetisyan, T. Bose, D. Gastler, D. Rankin, C. Richardson, J. Rohlf, L. Sulak, D. Zou

Brown University, Providence, USA
G. Benelli, D. Cutts, A. Garabedian, J. Hakala, U. Heintz, J.M. Hogan, K.H.M. Kwok, E. Laird, G. Landsberg, Z. Mao, M. Narain, J. Pazzini, S. Piperov, S. Sagir, R. Syarif, D. Yu

University of California, Davis, Davis, USA
R. Band, C. Brainerd, R. Breedon, D. Burns, M. Calderon De La Barca Sanchez, M. Chertok, J. Conway, R. Conway, P.T. Cox, R. Erbacher, C. Flores, G. Funk, M. Gardner, W. Ko, R. Lander, C. Mclean, M. Mulhearn, D. Pellett, J. Pilot, S. Shalhout, M. Shi, J. Smith, M. Squires, D. Stolp, K. Tos, M. Tripathi, Z. Wang

University of California, Los Angeles, USA
M. Bachtis, C. Bravo, R. Cousins, A. Dasgupta, A. Florent, J. Hauser, M. Ignatenko, N. Mccoll, D. Saltzberg, C. Schnaible, V. Valuev

University of California, Riverside, Riverside, USA
E. Bouvier, K. Burt, R. Clare, J. Ellison, J.W. Gary, S.M.A. Ghiasi Shirazi, G. Hanson, J. Heilman, P. Jandir, E. Kennedy, F. Lacroix, O.R. Long, M. Olmedo Negrete, M.I. Paneva, A. Shrinivas, W. Si, L. Wang, H. Wei, S. Wimpenny, B. R. Yates

University of California, San Diego, La Jolla, USA
J.G. Branson, S. Cittolin, M. Derdzinski, R. Gerosa, B. Hashemi, A. Holzner, D. Klein, G. Kole, V. Krutelyov, J. Letts, I. Macneill, M. Masciovecchio, D. Olivito, S. Padhi, M. Pieri, M. Sani, V. Sharma, S. Simon, M. Tadel, A. Vartak, S. Wasserbaech[63], J. Wood, F. Würthwein, A. Yagil, G. Zevi Della Porta

University of California, Santa Barbara - Department of Physics, Santa Barbara, USA
N. Amin, R. Bhandari, J. Bradmiller-Feld, C. Campagnari, A. Dishaw, V. Dutta, M. Franco Sevilla, C. George, F. Golf, L. Gouskos, J. Gran, R. Heller, J. Incandela, S.D. Mullin, A. Ovcharova, H. Qu, J. Richman, D. Stuart, I. Suarez, J. Yoo

California Institute of Technology, Pasadena, USA
D. Anderson, J. Bendavid, A. Bornheim, J.M. Lawhorn, H.B. Newman, T. Nguyen, C. Pena, M. Spiropulu, J.R. Vlimant, S. Xie, Z. Zhang, R.Y. Zhu

Carnegie Mellon University, Pittsburgh, USA
M.B. Andrews, T. Ferguson, T. Mudholkar, M. Paulini, J. Russ, M. Sun, H. Vogel, I. Vorobiev, M. Weinberg

University of Colorado Boulder, Boulder, USA
J.P. Cumalat, W.T. Ford, F. Jensen, A. Johnson, M. Krohn, S. Leontsinis, T. Mulholland, K. Stenson, S.R. Wagner

Cornell University, Ithaca, USA
J. Alexander, J. Chaves, J. Chu, S. Dittmer, K. Mcdermott, N. Mirman, J.R. Patterson, A. Rinkevicius, A. Ryd, L. Skinnari, L. Soffi, S.M. Tan, Z. Tao, J. Thom, J. Tucker, P. Wittich, M. Zientek

Fermi National Accelerator Laboratory, Batavia, USA
S. Abdullin, M. Albrow, G. Apollinari, A. Apresyan, A. Apyan, S. Banerjee, L.A.T. Bauerdick, A. Beretvas, J. Berryhill, P.C. Bhat, G. Bolla[†], K. Burkett, J.N. Butler, A. Canepa, G.B. Cerati, H.W.K. Cheung, F. Chlebana, M. Cremonesi, J. Duarte, V.D. Elvira, J. Freeman, Z. Gecse, E. Gottschalk, L. Gray, D. Green, S. Grünendahl, O. Gutsche, R.M. Harris, S. Hasegawa, J. Hirschauer, Z. Hu, B. Jayatilaka, S. Jindariani, M. Johnson, U. Joshi, B. Klima, B. Kreis, S. Lammel, D. Lincoln, R. Lipton, M. Liu, T. Liu, R. Lopes De Sá, J. Lykken, K. Maeshima, N. Magini, J.M. Marraffino, S. Maruyama, D. Mason, P. McBride, P. Merkel, S. Mrenna, S. Nahn, V. O'Dell, K. Pedro, O. Prokofyev, G. Rakness, L. Ristori, B. Schneider, E. Sexton-Kennedy, A. Soha, W.J. Spalding, L. Spiegel, S. Stoynev, J. Strait, N. Strobbe, L. Taylor, S. Tkaczyk, N.V. Tran, L. Uplegger, E.W. Vaandering, C. Vernieri, M. Verzocchi, R. Vidal, M. Wang, H.A. Weber, A. Whitbeck

University of Florida, Gainesville, USA
D. Acosta, P. Avery, P. Bortignon, D. Bourilkov, A. Brinkerhoff, A. Carnes, M. Carver, D. Curry, R.D. Field, I.K. Furic, J. Konigsberg, A. Korytov, K. Kotov, P. Ma, K. Matchev, H. Mei, G. Mitselmakher, D. Rank, D. Sperka, N. Terentyev, L. Thomas, J. Wang, S. Wang, J. Yelton

Florida International University, Miami, USA
Y.R. Joshi, S. Linn, P. Markowitz, J.L. Rodriguez

Florida State University, Tallahassee, USA
A. Ackert, T. Adams, A. Askew, S. Hagopian, V. Hagopian, K.F. Johnson, T. Kolberg, G. Martinez, T. Perry, H. Prosper, A. Saha, A. Santra, V. Sharma, R. Yohay

Florida Institute of Technology, Melbourne, USA
M.M. Baarmand, V. Bhopatkar, S. Colafranceschi, M. Hohlmann, D. Noonan, T. Roy, F. Yumiceva

University of Illinois at Chicago (UIC), Chicago, USA
M.R. Adams, L. Apanasevich, D. Berry, R.R. Betts, R. Cavanaugh, X. Chen, O. Evdokimov, C.E. Gerber, D.A. Hangal, D.J. Hofman, K. Jung, J. Kamin, I.D. Sandoval Gonzalez, M.B. Tonjes, H. Trauger, N. Varelas, H. Wang, Z. Wu, J. Zhang

The University of Iowa, Iowa City, USA
B. Bilki[64], W. Clarida, K. Dilsiz[65], S. Durgut, R.P. Gandrajula, M. Haytmyradov, V. Khristenko, J.-P. Merlo, H. Mermerkaya[66], A. Mestvirishvili, A. Moeller, J. Nachtman, H. Ogul[67], Y. Onel, F. Ozok[68], A. Penzo, C. Snyder, E. Tiras, J. Wetzel, K. Yi

Johns Hopkins University, Baltimore, USA
B. Blumenfeld, A. Cocoros, N. Eminizer, D. Fehling, L. Feng, A.V. Gritsan, P. Maksimovic, J. Roskes, U. Sarica, M. Swartz, M. Xiao, C. You

The University of Kansas, Lawrence, USA
A. Al-bataineh, P. Baringer, A. Bean, S. Boren, J. Bowen, J. Castle, S. Khalil, A. Kropivnitskaya,

D. Majumder, W. Mcbrayer, M. Murray, C. Royon, S. Sanders, E. Schmitz, J.D. Tapia Takaki, Q. Wang

Kansas State University, Manhattan, USA
A. Ivanov, K. Kaadze, Y. Maravin, A. Mohammadi, L.K. Saini, N. Skhirtladze, S. Toda

Lawrence Livermore National Laboratory, Livermore, USA
F. Rebassoo, D. Wright

University of Maryland, College Park, USA
C. Anelli, A. Baden, O. Baron, A. Belloni, B. Calvert, S.C. Eno, C. Ferraioli, N.J. Hadley, S. Jabeen, G.Y. Jeng, R.G. Kellogg, J. Kunkle, A.C. Mignerey, F. Ricci-Tam, Y.H. Shin, A. Skuja, S.C. Tonwar

Massachusetts Institute of Technology, Cambridge, USA
D. Abercrombie, B. Allen, V. Azzolini, R. Barbieri, A. Baty, R. Bi, S. Brandt, W. Busza, I.A. Cali, M. D'Alfonso, Z. Demiragli, G. Gomez Ceballos, M. Goncharov, D. Hsu, Y. Iiyama, G.M. Innocenti, M. Klute, D. Kovalskyi, Y.S. Lai, Y.-J. Lee, A. Levin, P.D. Luckey, B. Maier, A.C. Marini, C. Mcginn, C. Mironov, S. Narayanan, X. Niu, C. Paus, C. Roland, G. Roland, J. Salfeld-Nebgen, G.S.F. Stephans, K. Tatar, D. Velicanu, J. Wang, T.W. Wang, B. Wyslouch

University of Minnesota, Minneapolis, USA
A.C. Benvenuti, R.M. Chatterjee, A. Evans, P. Hansen, S. Kalafut, Y. Kubota, Z. Lesko, J. Mans, S. Nourbakhsh, N. Ruckstuhl, R. Rusack, J. Turkewitz

University of Mississippi, Oxford, USA
J.G. Acosta, S. Oliveros

University of Nebraska-Lincoln, Lincoln, USA
E. Avdeeva, K. Bloom, D.R. Claes, C. Fangmeier, R. Gonzalez Suarez, R. Kamalieddin, I. Kravchenko, J. Monroy, J.E. Siado, G.R. Snow, B. Stieger

State University of New York at Buffalo, Buffalo, USA
M. Alyari, J. Dolen, A. Godshalk, C. Harrington, I. Iashvili, D. Nguyen, A. Parker, S. Rappoccio, B. Roozbahani

Northeastern University, Boston, USA
G. Alverson, E. Barberis, A. Hortiangtham, A. Massironi, D.M. Morse, D. Nash, T. Orimoto, R. Teixeira De Lima, D. Trocino, D. Wood

Northwestern University, Evanston, USA
S. Bhattacharya, O. Charaf, K.A. Hahn, N. Mucia, N. Odell, B. Pollack, M.H. Schmitt, K. Sung, M. Trovato, M. Velasco

University of Notre Dame, Notre Dame, USA
N. Dev, M. Hildreth, K. Hurtado Anampa, C. Jessop, D.J. Karmgard, N. Kellams, K. Lannon, N. Loukas, N. Marinelli, F. Meng, C. Mueller, Y. Musienko[35], M. Planer, A. Reinsvold, R. Ruchti, G. Smith, S. Taroni, M. Wayne, M. Wolf, A. Woodard

The Ohio State University, Columbus, USA
J. Alimena, L. Antonelli, B. Bylsma, L.S. Durkin, S. Flowers, B. Francis, A. Hart, C. Hill, W. Ji, B. Liu, W. Luo, D. Puigh, B.L. Winer, H.W. Wulsin

Princeton University, Princeton, USA
S. Cooperstein, O. Driga, P. Elmer, J. Hardenbrook, P. Hebda, S. Higginbotham, D. Lange, J. Luo, D. Marlow, K. Mei, I. Ojalvo, J. Olsen, C. Palmer, P. Piroué, D. Stickland, C. Tully

University of Puerto Rico, Mayaguez, USA
S. Malik, S. Norberg

Purdue University, West Lafayette, USA
A. Barker, V.E. Barnes, S. Das, S. Folgueras, L. Gutay, M.K. Jha, M. Jones, A.W. Jung, A. Khatiwada, D.H. Miller, N. Neumeister, C.C. Peng, J.F. Schulte, J. Sun, F. Wang, W. Xie

Purdue University Northwest, Hammond, USA
T. Cheng, N. Parashar, J. Stupak

Rice University, Houston, USA
A. Adair, B. Akgun, Z. Chen, K.M. Ecklund, F.J.M. Geurts, M. Guilbaud, W. Li, B. Michlin, M. Northup, B.P. Padley, J. Roberts, J. Rorie, Z. Tu, J. Zabel

University of Rochester, Rochester, USA
A. Bodek, P. de Barbaro, R. Demina, Y.t. Duh, T. Ferbel, M. Galanti, A. Garcia-Bellido, J. Han, O. Hindrichs, A. Khukhunaishvili, K.H. Lo, P. Tan, M. Verzetti

The Rockefeller University, New York, USA
R. Ciesielski, K. Goulianos, C. Mesropian

Rutgers, The State University of New Jersey, Piscataway, USA
A. Agapitos, J.P. Chou, Y. Gershtein, T.A. Gómez Espinosa, E. Halkiadakis, M. Heindl, E. Hughes, S. Kaplan, R. Kunnawalkam Elayavalli, S. Kyriacou, A. Lath, R. Montalvo, K. Nash, M. Osherson, H. Saka, S. Salur, S. Schnetzer, D. Sheffield, S. Somalwar, R. Stone, S. Thomas, P. Thomassen, M. Walker

University of Tennessee, Knoxville, USA
A.G. Delannoy, M. Foerster, J. Heideman, G. Riley, K. Rose, S. Spanier, K. Thapa

Texas A&M University, College Station, USA
O. Bouhali[69], A. Castaneda Hernandez[69], A. Celik, M. Dalchenko, M. De Mattia, A. Delgado, S. Dildick, R. Eusebi, J. Gilmore, T. Huang, T. Kamon[70], R. Mueller, Y. Pakhotin, R. Patel, A. Perloff, L. Perniè, D. Rathjens, A. Safonov, A. Tatarinov, K.A. Ulmer

Texas Tech University, Lubbock, USA
N. Akchurin, J. Damgov, F. De Guio, P.R. Dudero, J. Faulkner, E. Gurpinar, S. Kunori, K. Lamichhane, S.W. Lee, T. Libeiro, T. Peltola, S. Undleeb, I. Volobouev, Z. Wang

Vanderbilt University, Nashville, USA
S. Greene, A. Gurrola, R. Janjam, W. Johns, C. Maguire, A. Melo, H. Ni, P. Sheldon, S. Tuo, J. Velkovska, Q. Xu

University of Virginia, Charlottesville, USA
M.W. Arenton, P. Barria, B. Cox, R. Hirosky, M. Joyce, A. Ledovskoy, H. Li, C. Neu, T. Sinthuprasith, Y. Wang, E. Wolfe, F. Xia

Wayne State University, Detroit, USA
R. Harr, P.E. Karchin, J. Sturdy, S. Zaleski

University of Wisconsin - Madison, Madison, WI, USA
M. Brodski, J. Buchanan, C. Caillol, S. Dasu, L. Dodd, S. Duric, B. Gomber, M. Grothe, M. Herndon, A. Hervé, U. Hussain, P. Klabbers, A. Lanaro, A. Levine, K. Long, R. Loveless, G.A. Pierro, G. Polese, T. Ruggles, A. Savin, N. Smith, W.H. Smith, D. Taylor, N. Woods

†: Deceased

1: Also at Vienna University of Technology, Vienna, Austria

2: Also at State Key Laboratory of Nuclear Physics and Technology, Peking University, Beijing, China

3: Also at Universidade Estadual de Campinas, Campinas, Brazil

4: Also at Universidade Federal de Pelotas, Pelotas, Brazil

5: Also at Université Libre de Bruxelles, Bruxelles, Belgium

6: Also at Institute for Theoretical and Experimental Physics, Moscow, Russia

7: Also at Joint Institute for Nuclear Research, Dubna, Russia

8: Also at Suez University, Suez, Egypt

9: Now at British University in Egypt, Cairo, Egypt

10: Now at Helwan University, Cairo, Egypt

11: Also at Université de Haute Alsace, Mulhouse, France

12: Also at Skobeltsyn Institute of Nuclear Physics, Lomonosov Moscow State University, Moscow, Russia

13: Also at Ilia State University, Tbilisi, Georgia

14: Also at CERN, European Organization for Nuclear Research, Geneva, Switzerland

15: Also at RWTH Aachen University, III. Physikalisches Institut A, Aachen, Germany

16: Also at University of Hamburg, Hamburg, Germany

17: Also at Brandenburg University of Technology, Cottbus, Germany

18: Also at MTA-ELTE Lendület CMS Particle and Nuclear Physics Group, Eötvös Loránd University, Budapest, Hungary

19: Also at Institute of Nuclear Research ATOMKI, Debrecen, Hungary

20: Also at Institute of Physics, University of Debrecen, Debrecen, Hungary

21: Also at Indian Institute of Technology Bhubaneswar, Bhubaneswar, India

22: Also at Institute of Physics, Bhubaneswar, India

23: Also at University of Visva-Bharati, Santiniketan, India

24: Also at University of Ruhuna, Matara, Sri Lanka

25: Also at Isfahan University of Technology, Isfahan, Iran

26: Also at Yazd University, Yazd, Iran

27: Also at Plasma Physics Research Center, Science and Research Branch, Islamic Azad University, Tehran, Iran

28: Also at Università degli Studi di Siena, Siena, Italy

29: Also at INFN Sezione di Milano-Bicocca; Università di Milano-Bicocca, Milano, Italy

30: Also at Purdue University, West Lafayette, USA

31: Also at International Islamic University of Malaysia, Kuala Lumpur, Malaysia

32: Also at Malaysian Nuclear Agency, MOSTI, Kajang, Malaysia

33: Also at Consejo Nacional de Ciencia y Tecnología, Mexico city, Mexico

34: Also at Warsaw University of Technology, Institute of Electronic Systems, Warsaw, Poland

35: Also at Institute for Nuclear Research, Moscow, Russia

36: Now at National Research Nuclear University 'Moscow Engineering Physics Institute' (MEPhI), Moscow, Russia

37: Also at Institute of Nuclear Physics of the Uzbekistan Academy of Sciences, Tashkent, Uzbekistan

38: Also at St. Petersburg State Polytechnical University, St. Petersburg, Russia

39: Also at University of Florida, Gainesville, USA

40: Also at P.N. Lebedev Physical Institute, Moscow, Russia

41: Also at California Institute of Technology, Pasadena, USA

42: Also at Budker Institute of Nuclear Physics, Novosibirsk, Russia

43: Also at Faculty of Physics, University of Belgrade, Belgrade, Serbia
44: Also at University of Belgrade, Faculty of Physics and Vinca Institute of Nuclear Sciences, Belgrade, Serbia
45: Also at Scuola Normale e Sezione dell'INFN, Pisa, Italy
46: Also at National and Kapodistrian University of Athens, Athens, Greece
47: Also at Riga Technical University, Riga, Latvia
48: Also at Universität Zürich, Zurich, Switzerland
49: Also at Stefan Meyer Institute for Subatomic Physics (SMI), Vienna, Austria
50: Also at Gaziosmanpasa University, Tokat, Turkey
51: Also at Istanbul Aydin University, Istanbul, Turkey
52: Also at Mersin University, Mersin, Turkey
53: Also at Cag University, Mersin, Turkey
54: Also at Piri Reis University, Istanbul, Turkey
55: Also at Izmir Institute of Technology, Izmir, Turkey
56: Also at Necmettin Erbakan University, Konya, Turkey
57: Also at Marmara University, Istanbul, Turkey
58: Also at Kafkas University, Kars, Turkey
59: Also at Istanbul Bilgi University, Istanbul, Turkey
60: Also at Rutherford Appleton Laboratory, Didcot, United Kingdom
61: Also at School of Physics and Astronomy, University of Southampton, Southampton, United Kingdom
62: Also at Instituto de Astrofísica de Canarias, La Laguna, Spain
63: Also at Utah Valley University, Orem, USA
64: Also at Beykent University, Istanbul, Turkey
65: Also at Bingol University, Bingol, Turkey
66: Also at Erzincan University, Erzincan, Turkey
67: Also at Sinop University, Sinop, Turkey
68: Also at Mimar Sinan University, Istanbul, Istanbul, Turkey
69: Also at Texas A&M University at Qatar, Doha, Qatar
70: Also at Kyungpook National University, Daegu, Korea